Transcranial direct current stimulation modulates primate brain dynamics across states of consciousness

Guylaine Hoffner[1*#], Pablo Castro[1,2*], Lynn Uhrig[1,3], Camilo Miguel Signorelli[4,5,6], Morgan Dupont[1], Jordy Tasserie[7], Alain Destexhe[2], Rodrigo Cofre[2,8], Jacobo Sitt[9+] and Bechir Jarraya[1,10+#].

*Co-first authors
[+]Co-last authors
[#]Corresponding authors: guylaine.hoffner@inserm.fr (GH); bechir.jarraya@cea.fr (BJ)

Affiliations

[1]Cognitive Neuroimaging Unit, CEA, INSERM, Université Paris-Saclay, NeuroSpin Center, 91191 Gif-sur-Yvette, France
[2]Institute of Neuroscience (NeuroPSI), Paris-Saclay University, Centre National de la Recherche Scientifique (CNRS), Gif-sur-Yvette, France
[3]Department of Anesthesiology and Critical Care, Necker Hospital, AP-HP, Université de Paris Cité, Paris, France
[4]Department of Computer Science, University of Oxford, Oxford, 7 Parks Rd, Oxford OX1 3QG
[5] Laboratory of Neurophysiology and Movement Biomechanics (LNMB), Université Libre de Bruxelles (ULB), Route de Lennik 808, CP 640, Building N, campus Erasme, 1070 Brussels
[6] Center for Philosophy of Artificial Intelligence, University of Copenhagen, Karen Blixens Plads 8, Copenhagen 2300, Denmark.
[7]Center for Brain Circuit Therapeutics, Department of Neurology, Brigham & Women's Hospital, Harvard Medical School, Boston, MA, USA
[8]Laboratoire de Physique de l'École Normale Supérieure, CNRS, PSL University, Sorbonne Université and Université Paris Cité, 75005 Paris, France
[9]Sorbonne Université, Institut du Cerveau - Paris Brain Institute - ICM, Inserm, CNRS, Paris 75013, France
[10]Department of Neurology, Hopital Foch, 92150, Suresnes, France

Graphical Abstract

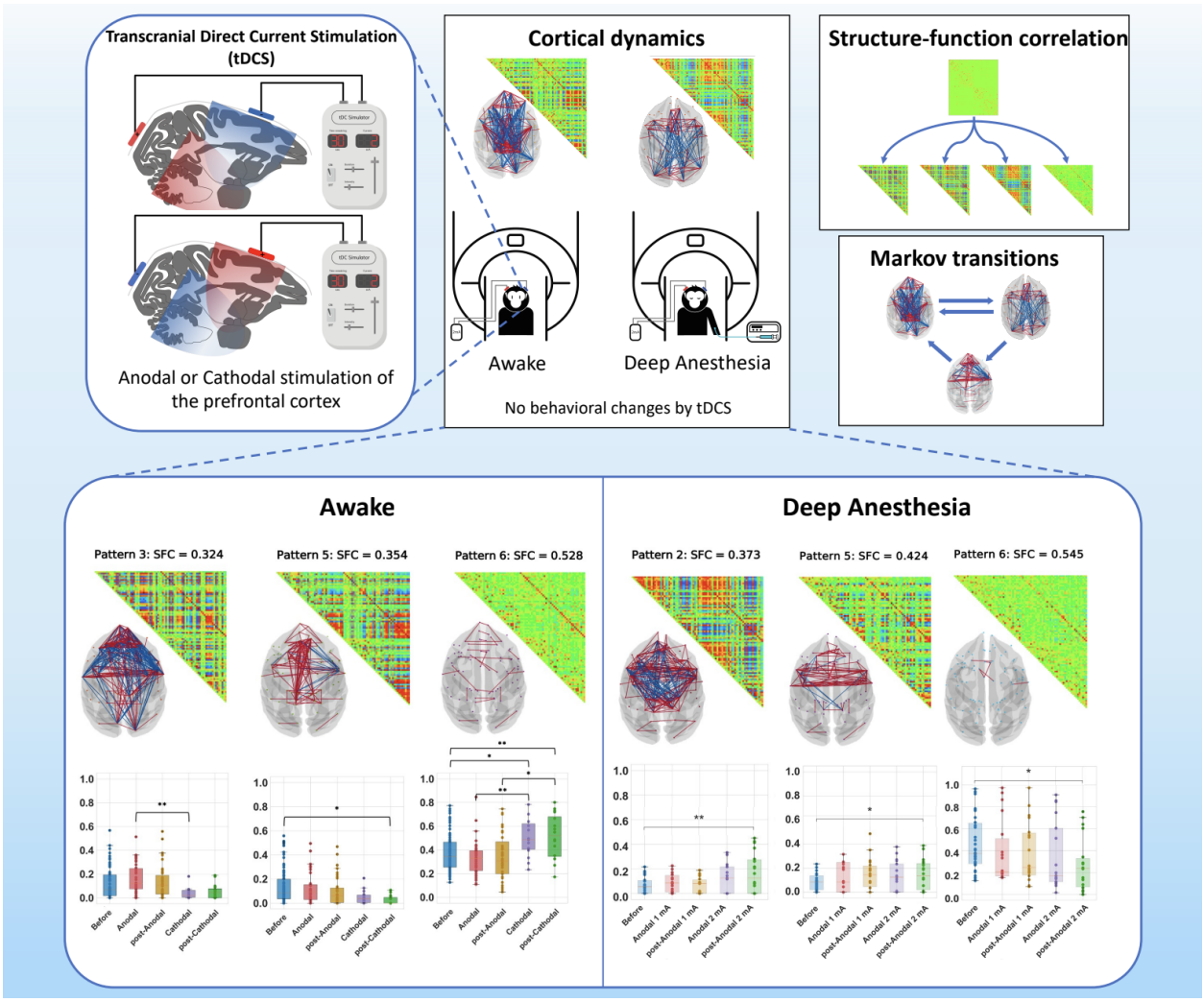

Abstract

Background: Transcranial direct current stimulation (tDCS) is a non-invasive neuromodulation approach that has been reported to perturb task activity and to benefit patients with a variety of diseases. Nevertheless, the effects of tDCS on brain dynamics and transitions in brain patterns across states of consciousness remain poorly understood.

Objective: Here, we investigated the modulatory effect of prefrontal cortex (PFC) tDCS on brain dynamics, both in the awake state and during anesthesia-induced loss of consciousness in non-human primates.

Methods: We acquired functional magnetic resonance imaging (fMRI) data before, during, and after the application of high-density tDCS (HD-tDCS) utilizing a prefrontal-occipital montage with two electrodes. In the awake state, macaques received either anodal or cathodal PFC stimulation. Under anesthesia, macaques underwent two consecutive anodal PFC stimulations of increasing intensity. Dynamical functional connectivity was measured using fMRI, and the resulting connectivity matrices were clustered into distinct 'brain patterns'.

Results: We found that cathodal PFC HD-tDCS robustly disrupted the rich dynamic repertoire of brain patterns of the awake state. It increased the brain structure-function correlation, decreased Shannon entropy, and strongly favored Markov chain transition probabilities towards patterns closest to anatomy. Under anesthesia, 2 mA anodal PFC HD-tDCS significantly changed the distribution of brain patterns and reduced the structure-function correlation.

Conclusion: Our findings offer compelling evidence that prefrontal tDCS induces a striking modification in the fMRI-based dynamic organization of the brain across varying states of consciousness. This contributes to an enhanced understanding of the neural mechanisms underlying tDCS neuromodulation.

Keywords: high-density tDCS, fMRI, functional connectivity, brain dynamics, consciousness, prefrontal cortex.

INTRODUCTION

Transcranial direct current stimulation (tDCS) is a non-invasive electrical brain stimulation technique involving the application of a weak current through two or more electrodes placed on the scalp (Lefaucheur and Wendling 2019). While conventional tDCS relies on the use of relatively large rectangular pad electrodes, a more recent approach, called high-density tDCS (HD-tDCS), utilizes more compact ring electrodes, allowing for increased focality, stronger electric fields, and presumably, greater neurophysiological changes and longer-lasting after-effects (Datta et al. 2009; Dmochowski et al. 2011; Kuo et al. 2013; Gbadeyan et al. 2016). In vivo and in vitro data suggest that tDCS acts through diverse, concurrent, and multiscale modes of action, ranging from membrane polarization, spike timing, synaptic plasticity, de novo protein expression, cellular morphological changes, white and grey matter microstructure modifications, to functional network synchronization (Lefaucheur et al. 2017; Cirillo et al. 2017; Lefaucheur and Wendling 2019; Barbati, Podda, and Grassi 2022; Antonenko et al. 2023). The ongoing neural activity during tDCS administration is likely to exert a crucial influence, given that tDCS effects have been reported to be state-dependent, primarily modulating active networks (Antal et al., 2007; Bikson, Name, and Rahman, 2013; Li et al., 2019).

A decade ago, anodal tDCS of the left dorsolateral prefrontal cortex (DLPFC) was reported to promote clinical improvements in patients with disorders of consciousness (DOCs) (Thibaut et al. 2014; Angelakis et al. 2014). Subsequently, many clinical trials have been conducted and supported these initial findings (e.g. (Thibaut et al. 2017; Y. Zhang et al. 2017; Martens et al. 2018; Cavinato et al. 2019; Wu et al. 2019; Hermann et al. 2020; Peng et al. 2022; Thibaut et al. 2023)). Other clinical trials have begun to explore the outcomes of stimulating other brain regions, such as the motor cortex (Martens et al. 2019; Straudi et al. 2019) or the parietal cortex (W. Huang et al. 2017; Guo et al. 2019; C. Zhang et al. 2022; Wan et al. 2023). Analysis of resting-state functional magnetic resonance imaging (rs-fMRI) data provided evidence that an increase in functional connectivity (FC) can be induced by tDCS in some DOCs patients, both at the site of stimulation and in remote regions (Peng et al. 2022). Similar findings have been reported

in patients with neurological disorders, such as schizophrenia or primary progressive aphasia (Chan and Han 2020), and in healthy humans, with FC strengthening observed between frontal and parietal, temporal and parieto-occipital regions (Keeser et al. 2011; Peña-Gómez et al. 2012; Mondino et al. 2019; Leaver et al. 2022; Bouchard, Renauld, and Fecteau 2023).

On another hand, anesthesia is a valuable model for exploring the mechanisms of loss of consciousness. Interestingly, it has been speculated that tDCS may represent a novel strategy to accelerate recovery from general anesthesia (Kato and Solt 2021), based on a study in rats showing that repeated stimulation of the motor cortex facilitates the return of the righting reflex and visual and working memory after isoflurane anesthesia (Mansouri and García 2021). However, the effects of tDCS on brain activity while sedated remain largely unexplored.

The brain's spontaneous activity can be assessed using rs-fMRI, a technique in which fMRI data is collected while the subject is not engaged in a specific task (B. B. Biswal 2012; B. Biswal et al. 1995; Allen et al. 2014; Cabral et al. 2017; Cornblath et al. 2020). According to this approach, the brain seems to dynamically transit through various ephemeral configurations, thought to support specific cognitive functions (Deco, Jirsa, and McIntosh 2013; Shine et al. 2016; Lurie et al. 2020; Fox et al. 2006; Vincent et al. 2006; Damoiseaux et al. 2006; De Luca et al. 2005; Raichle et al. 2001; Calhoun et al. 2014; Preti, Bolton, and Van De Ville 2017; Baker et al. 2014; Deco, Jirsa, and McIntosh 2011). Moreover, wakefulness and unconsciousness induced by different anesthetics have been associated with distinct transient brain patterns in terms of their sequence and occurrence in non-human primates (NHPs) (Barttfeld et al. 2015; Uhrig et al. 2018). This finding has been confirmed in humans and generalized to various contexts of loss of consciousness, whether in patients with impaired consciousness, under anesthesia or during sleep (Luppi et al. 2021; Z. Huang et al. 2020; Demertzi et al. 2019a; Castro et al. 2023; Golkowski et al. 2019). Altogether, these studies revealed that the conscious brain is traversed by a rich and mobile set of functional brain patterns that deviate from anatomical connectivity. In contrast, the unconscious brain, regardless of the cause of

loss of consciousness, is characterized by a smaller number and stiffer transient functional patterns that more closely follow anatomical connectivity. These different structure-function configurations have been proposed as signatures of consciousness and unconsciousness, respectively.

Interestingly, a recent rs-fMRI study has started to examine whether tDCS can alter dynamic brain activity in healthy humans (Tu et al., 2021). Using the co-activation pattern (CAP) method and the DLPFC as a seed, it was shown that the stimulation can perturb both occurrences and transitions of some CAPs. While these data suggest that some elements of brain dynamics may be influenced by tDCS, it would be of great interest to investigate whether tDCS can induce changes in these dynamic signatures in other models of loss of consciousness, such as anesthesia, or whether the stimulation could disturb wakeful dynamic signatures.

Here, we focused on determining whether prefrontal HD-tDCS can modify the relationship between the structural and functional brain organization in fMRI signals in NHPs, either in the awake state or under deep propofol anesthesia. Our specific aims were to determine the effects of prefrontal HD-tDCS on brain dynamics 1) in awake NHPs receiving either anodal or cathodal stimulation, 2) in anesthetized NHPs receiving anodal stimulation at two different intensity levels, and 3) the time course of these putative changes relative to the stimulation (i.e., during and after the stimulation). Our results provided evidence that anodal prefrontal HD-tDCS only marginally affected the brain dynamics in awake animals. In contrast, cathodal prefrontal HD-tDCS significantly reorganized the functional repertoire in favor of anatomically similar brain states without apparent behavioral modification. In addition, both anodal and cathodal stimulation affected Markov chain transitions between brain states, with some changes specific to ongoing stimulation and others to post-stimulation. Under anesthesia, anodal prefrontal HD-tDCS delivered at an intensity of 2 mA, but not 1 mA, significantly reduced the structure-function correlation but did not restore the broad and rich dynamic repertoire of functional states that is a hallmark of wakefulness, nor induce signs of arousal in the animals.

MATERIAL AND METHODS

Animals

Four rhesus monkeys (Macaca mulatta, 18-20 years, 7.2-9.8 kg) were scanned. Two males were tested for the awake experiments (monkeys J and Y), and one female and one male were tested for experiments under anesthesia (monkeys R and N).

All procedures follow the European Convention for Animal Care (86-406) and the National Institutes of Health's Guide for the Care and Use of Laboratory Animals. Animal studies were approved by the Institutional Ethical Committee (CETEA protocol #16-040).

tDCS protocol

We applied HD-tDCS using a battery-powered stimulator (1x1 tES device, Soterix medical) located outside the scanner room, and a complete MR-compatible setup, consisting of an MRI filter, carbon composition cables, and two high-density (HD) carbon rubber electrodes inserted into HD-tES MRI electrode holders (Soterix medical). Electrode contact quality was checked before all stimulation sessions by using the Pre-stim Tickle function of the device (1 mA for 30 s). If a poor contact was detected, the electrode-scalp contact was readjusted and/or the conductive paste or gel was added to improve contact quality. Electrode contact quality was continuously monitored during the stimulation.

To reduce the likelihood of the monkeys experiencing discomfort at the electrode sites, the current was gradually increased from 0 mA to the target intensity over the first 30 seconds. The current was also gradually decreased to 0 mA over the last 30 seconds of each tDCS stimulation period. The tDCS device was turned off during the acquisition of the pre- and post-stimulation fMRI blocks to avoid any hypothetical biological effect of the residual current (Fonteneau et al. 2019), which we measured to be 0.023 mA. After the

tDCS-fMRI scanning sessions, the monkeys' scalps were examined for any redness, skin burns, or other lesions. None of the monkeys showed any side effects.

Awake experiments

In the awake experiments, elastic bands with fasteners were used to secure the electrode holders in place. We used a conductive and adhesive paste (Ten20 conductive paste, Weaver and Company) to ensure consistent electrode-skin contact. The anode electrode was placed over the left PFC (F3) and the cathode electrode over the right occipital cortex (O2), or the reverse montage was employed, with the cathode electrode placed over the right PFC (F4) and the anode over the left occipital cortex (O1). We used monkey EEG caps (EasyCap, 13 channels, Fp1, Fp2, F3, F4, T3, T4, P3, P4, O1, O2, Oz, reference electrode, ground electrode), based on the international 10-20 EEG system, to obtain F3, F4, O1, and O2 locations, where we placed the stimulation electrodes. The two montages were respectively abbreviated F4/O1 and O1/F4. tDCS was delivered for 20 min at a current intensity of 2 mA.

Anesthesia experiments

For anesthesia experiments, the electrode holders were held in place with Monkey-2D caps (EasyCaps GmbH), using an EEG gel to obtain low impedance (One Step EEG gel, Germany) as the conductive medium. Monkey R was stimulated with an F3/O2 montage (anodal electrode over the left PFC and cathodal electrode over the right occipital cortex) and monkey N was stimulated with an F4/O1 montage (anodal electrode over the right PFC and cathodal electrode over the left occipital cortex). This different, but still close placement of the electrodes between the two animals, was dictated by constraints related to the location of the headpost (with the cement used to anchor the headpost spreading more or less asymmetrically) and the anatomy/specificity of each animal's head. Because of the small size of the monkey's head, we expected that tDCS stimulation with these two symmetrical montages would result in nearly equivalent electric fields across the monkey’s head and produce roughly similar effects on brain activity. Two 20-minute blocks of tDCS stimulation were applied consecutively in each scanning session, with a current intensity of 1 mA for the first block and 2 mA for the second block (Figure 1).

fMRI data acquisition

The monkeys were scanned on a 3-T horizontal scanner (Siemens Prisma Fit, Erlanger, Germany) with a custom-built single transmit-receiver surface coil. The parameters of the fMRI sequences were as follows: (i) functional scan: EPI, TR = 2400 ms, TE = 20 ms, 1.5-mm isotropic voxel size, and 111 brain volumes per run, (ii) anatomical scan: MPRAGE, T1-weighted, TR = 2200 ms, TE = 3,18 ms, 0.80-mm isotropic voxel size, sagittal orientation. Prior to each scanning session, monocrystalline iron oxide nanoparticles (10 mg/kg, i.v.; MION, Feraheme, AMAG Pharmaceuticals, MA) were injected into the saphenous vein of the monkey to improve the contrast-to-noise ratio and the spatial selectivity of the MR signal changes (Vanduffel et al., Neuron 2001).

All fMRI data were acquired while the monkeys were engaged in a passive event-related auditory task, the local-global paradigm, based on local and global deviations from temporal regularities (Bekinschtein et al., PNAS 2009; Uhrig et al., 2014). The investigation of how tDCS perturbs cerebral responses to local and global deviants will be analyzed later and is not shown in this paper. fMRI data were acquired before tDCS stimulation, during tDCS stimulation (onset of fMRI acquisition starting after the ramp-up period and stopping before the ramp-down period), and after tDCS stimulation. For anesthesia experiments, a second round of stimulation/post-stimulation block was completed (see below). Four runs of 111 brain volumes were acquired during each condition (before tDCS stimulation, during tDCS stimulation and after tDCS stimulation). Finally, all sessions ended up with an anatomical scan.

Awake protocol

Monkeys were implanted with an MR-compatible headpost, trained to sit in a sphinx position in a primate chair and to fixate within a 2×2° window centred on a red dot (0.35×0.35°) within a “mock” MR bore before being scanned. fMRI data were acquired in awake macaques as previously described (Uhrig, Dehaene, and Jarraya 2014). The eye position was monitored at 120 Hz (Iscan Inc., MA, USA) and the fixation rate during the

fMRI run was recorded (Sup. Table 1). No physiological parameters were recorded in the awake state.

A total of 288 runs were acquired in the awake state: 136 runs before stimulation, 56 runs during anodal stimulation, 56 runs after anodal stimulation, 20 runs during cathodal stimulation, and 20 runs after cathodal stimulation (see Sup. Table 1 for details of the number of runs acquired per monkey).

Anesthesia protocol

The anesthesia protocol is described in detail in a previous study (Tasserie et al. 2022). Anesthesia was induced with an intramuscular injection of ketamine (10mg/kg, Virbac, France) and dexmedetomidine (20 microgr/kg, Ovion Pharma, USA) and maintained with a target-controlled infusion (TCI) (Alaris PK Syringe pump, CareFusion, CA, USA) of propofol (Panpharma Fresenius Kabi, France) using the “Paedfusor” pharmacokinetic model (Absalom and Kenny, 2005;) (Monkey R: TCI 5.8 micrgr/ml, Monkey N: TCI 4.3 micrgr/m). Monkeys were intubated and mechanically ventilated. The physiological parameters (heart rate, noninvasive blood pressure, oxygen saturation, respiratory rate, end-tidal carbon dioxide and skin temperature) were monitored (Maglife, Schiller, France) and recorded (Sup. Table 3). A muscle-blocking agent (cisatracurium, GlaxoSmithKline, France, 0.15 mg/kg, bolus i.v., followed by a continuous infusion rate of 0.18mg/kg/h) was used during all anesthesia fMRI sessions to avoid artifacts.

We referred to a clinical arousal scale at the beginning and end of each scanning session to characterize the behavior of monkeys in experiments under anesthesia. This scale comprises several indicators: exploration of the environment, spontaneous movements, shaking/prodding, toe pinch, eye-opening, and corneal reflex (for more details see (Uhrig et al. 2016; Tasserie et al. 2022).

A total of 136 runs were acquired under anesthesia: 40 runs before stimulation, 24 runs during 1 mA anodal stimulation, 24 runs after 1 mA anodal stimulation, 24 runs during 2

mA anodal stimulation and 24 runs after 2 mA anodal stimulation (see Sup. Table 1 for details of the number of runs acquired per monkey).

Statistical analysis of the physiological data

One-way analysis of variance (ANOVA) was used to compare the effect of the stimulation on mean heart rate, blood pressure and other vital parameters under anesthesia. Statistical analysis and multiple comparisons were performed using home-made MATLAB scripts (MathWorks, USA), with a statistical threshold of $p < 0.05$, Bonferroni-corrected.

fMRI data analyses

fMRI preprocessing

Functional images were reoriented, realigned, resampled (1 mm isotropic), smoothed (Gaussian kernel, 3 mm full width at half maximum) and rigidly co-registered to the anatomical template of the monkey MNI space (Frey et al. 2011) using custom-made scripts (Uhrig, Dehaene, and Jarraya 2014).

The global signal was regressed out from the images to remove any confounding effects due to physiological changes (e.g., respiratory or cardiac variations). Voxel time series were filtered with a low-pass (0.05 Hz cutoff) and high-pass (0.0025 Hz cutoff) filters and a zero-phase fast Fourier notch filter (0.03 Hz) to remove an artifactual pure frequency present in all the data (Barttfeld et al. 2015; Uhrig et al. 2018).

An additional cleaning step was performed to check the quality of the data after time series extraction, as described previously (Signorelli et al., 2021). The procedure was based on a trial-by-trial visual inspection, by an expert neuroimager, of the time series for all nodes, the Fourier transform of each signal, the functional connectivity for each subject, and the dynamical connectivity computed with phase correlation. For each dataset, visual inspection was first used to become familiar with the characteristics of the

entire dataset: how the amplitude spectrum, time series, FC and dynamic FC look. Subsequently, each trial was inspected again with a particular focus on two main types of potential artefacts. The first one corresponds to potential issues with the acquisition and is given by stereotyped sinusoidal oscillatory patterns without variation. The second one refers to potential head or other movement not fully corrected by our preprocessing procedure. This last artefact can be sometimes recognized by bursts or peaks of activity. Sinusoidal activity generates artificially high functional correlation and peak of frequencies in the amplitude spectrum plot. Uncorrected movements generate peaks of activity with high functional correlation and sections of high functional correlations in the dynamical FC matrix. If we observed any of these anomalies we rejected the trial, opting to adopt a conservative policy. Trials were retained if the row signal showed no evidence of artifactual activity, the functional connectivity was coherent with the average and the dynamical connectivity showed consistent patterns over time.

Finally, a total of 295 runs were analyzed in the following conditions: awake state, 190 runs (before HD-tDCS, 82 runs; during anodal HD-tDCS, 38 runs, after anodal HD-tDCS, 39 runs, during cathodal HD-tDCS, 15 runs, after cathodal HD-tDCS, 16 runs) and anesthesia, 105 runs (before HD-tDCS, 34 runs; during 1 mA anodal HD-tDCS, 18 runs; after 1 mA anodal HD-tDCS, 18 runs; during 2 mM anodal HD-tDCS, 17 runs; after 2 mA anodal HD-tDCS, 18 runs).

Anatomical parcellation and structural connectivity

Anatomical connectivity data were obtained from a recent macaque connectome generated by coupling diffusion MRI tractography with axonal tract tracing studies (Bakker, Wachtler, and Diesmann 2012; Shen et al. 2019). The macaque cortex was subdivided using the Regional Map parcellation method (Kötter and Wanke 2005). The parcellation includes 82 cortical regions of interest (41 ROIs per hemisphere). Structural (i.e., anatomical) connectivity data are represented as matrices in which the 82 cortical regions of interest are plotted on the x-axis and y-axis. The CoComac connectivity matrix contains information about the strength of the connections between cortical areas, with each cell representing the connection between any two regions.

Signals representation

Given a real-valued signal $x(t)$, there exists a unique analytic representation $\tilde{x}(t)$, which is a complex signal, with the same Fourier transform as the real-valued signal strictly defined for positive frequencies. This analytic signal can be constructed from the real-valued signal using the Hilbert transform H:

$$\tilde{x}(t) = x(t) + iH[x(t)]$$

i being the squared root of -1, the imaginary unit. The motivations for using the analytic signal are that, given some real-value data (i.e. MION signals), one can determine two functions of time that provide more meaningful properties of the signal. For a narrowband signal that can be written as an amplitude-modulated low-pass signal $A(t)$ with carrier frequency expressed by $\varphi(t)$:

$$x(t) = A(t)\cos[\varphi(t)].$$

Then, if the Fourier transforms of $A(t)$ and $\cos[\varphi(t)]$ have separate supports, the analytic signal of a narrowband signal can be rewritten as the product of two meaningful components

$$\tilde{x}(t) = A(t)e^{i\varphi(t)}.$$

Where $A(t)$ is the instantaneous amplitude, $\varphi(t)$ the instantaneous phase obtained from the Hilbert transform $H[x(t)]$.

The narrower the bandwidth of the signal of interest, the better the Hilbert transform produces an analytic signal with a meaningful envelope and phase (Glerean et al. 2012). Adopting a band-pass filtered version of the MION time series improves the separation between the phase and envelope spectra. The time series were z-scored, and subsequently, the Hilbert transform was computed to obtain the phase of each signal at each volume and each moment (TR, i.e. one-time sample).

Phase-based dynamic functional coordination

A recurrent issue in fMRI studies dealing with dynamical analysis is the arbitrary choices in the time-windows length and their overlapping when capturing temporal oscillations through a sliding-window methodology (Hindriks et al. 2016; Xie et al. 2019; Allen et al. 2014; Barttfeld et al. 2015). Thus, phase-based dynamic functional coordination was preferred (Alonso Martínez et al. 2020; Cabral et al. 2017; Vohryzek et al. 2020; Demertzi et al. 2019a). Analytic representations of signals were employed to derive a phase signal corresponding to the MION time series. We computed the instantaneous phase $\varphi_n(t)$ of the signals across all regions of interest (ROI) $n \in \{1, ..., N\}$ for each repetition time (TR) $t \in \{2, \ldots, T-1\}$. The first and last repetition time (TR) of each fMRI scan were excluded due to possible signal distortions induced by the Hilbert transform (Bracewell 2000).

The instantaneous phase was computed using Euler's formula from the analytic signal, which was then "enfolded" within the range of $-\pi$ to π, facilitating the calculation of inter-ROI phase differences. To obtain a whole-brain pattern of phase differences, the phase coherence between pairs of areas k and j at each time t, labeled $PC(k, j, t)$, was estimated using the pairwise phase coherence defined as the cosinus of the angular difference:

$$PC(k, j, t) = \cos(\varphi_k(t) - \varphi_j(t)).$$

When areas k and j have synchronized MION signals at time t, the phase coherence takes the value 1, and when areas k and j are in anti-phase at time t, their associated phase coherence is -1. All the intermediate cases lie in between the interval $[-1, 1]$. This computation was repeated for all subjects. For each subject, the resulting phase coherence was a three-dimensional tensor with dimension $N \times N \times T$, where N is the total number of regions in the parcellation (here 82 regions) and T the total number of TR in each fMRI session. One can easily see the symmetry with respect to the spatial dimensions ($PC(k, j, t) = PC(j, k, t)$). Hence, only the triangular superior parts of the phase coherence matrices were used for later computations, thus reducing the phase

space's size to $\frac{N \times (N-1)}{2}$ (the diagonal was omitted) and containing the useful available information.

K-Means clustering

To assess recurring coordination patterns among individuals in both datasets, a multistep methodology was employed. First, the scanning sessions were transformed into matrices, wherein one dimension represented instantaneous phase differences (feature space), as explained above, and the other dimension represented time. We concatenate all the vectorized triangular superior parts for all subjects at all times and from the experimental conditions, hence obtaining phase-spaces over time matrices, one for each condition. Each of the resulting matrices were subjected to the k-means clustering algorithm utilizing the L2 "Euclidean" distance metric. This resulted in a discrete set of k coordination patterns and their corresponding occurrence over time.

This process yielded k cluster centroids, which served as representatives of the recurring coordination patterns, accompanied by a label indicating the closest pattern for each instantaneous phase difference at every given TR.

The number of clusters was determined for a range $k = \{3, ..., 10\}$, with 100 initializations and 300 iterations each, using the 'k-means++' initialization method, respectively to ensure respectively a maximum (or minimum) value for various metrics used as a proxy for choosing the optimal k-number of clusters, and for the stability in the centroids obtained. To determine the most appropriate number of clusters, we employed the inter-pattern correlation variance (IPCV) as the primary method as we are mainly interested in computing approximately correct centroids, supplemented by the elbow method for confirmation.

The IPCV is computed by vectorizing the set of centroids for a given k and calculating the variance of Pearson correlations between each pair of centroids (Demertzi et al. 2019a). The optimal k, indicating the number of clusters, is determined by identifying the

maximum value of this metric. To validate this optimal k, we employed the elbow method, which is typically based on the within-cluster sum of squares differences. While the elbow was not always as distinctly observable as desired, it still often coincided with the proposed k from the IPCV.

Structure-function correlation

To investigate the dependence of brain dynamics on the state of consciousness, we defined a measure of similarity between functional and structural connectivity. We resorted to a widely used group estimate of macaque anatomical connectivity provided by the CoCoMac 2.0 database. We computed the linear correlation coefficient between the entries of both matrices (k-means centroids and anatomical connectome) for each set of k-clusters. This was performed for each phase-based coordination pattern obtained using the k-means algorithm and was denoted structure-function correlation (SFC). We then reorganized the patterns' labels, their unique associated integer between 1 and k, such that the new 'first' pattern, would be the pattern with the lowest SFC, and the 'k^{th}' pattern the one with the highest correlation to the anatomy (i.e. structure). Last, we computed the linear slope coefficient of the relationship between the occurrence rate of each centroid and the corresponding centroid/anatomical correlation (i.e. the SFC) to establish a possible tendency for functional states with higher (or lower) correlation to the anatomy.

Brain states' presence rate distribution and Shannon Entropy

For each condition, we computed the histogram associated with the total time of visits of each pattern. This histogram, after normalization, corresponds to the probability distribution of the patterns' occurrence. For each of the normalized histogram of occurrence, and each value of k in the k-means algorithm, we obtained the Shannon entropy (Shannon 1948) as follows:

$$S = -\sum_i P_i \log_2 P_i$$

Where P_i is the probability (normalized histogram) of visit for each pattern in each brain state (condition).

Markov Chain

For every TR, the k-means algorithm assigns the index of the closest centroid to the corresponding empirical phase coherence matrix, resulting in a sequence of indexes (integers, between 1 and k). We reckon the sequence of "patterns visited" as a sequence of random variables that jumps from one pattern to another pattern with a certain probability given by the empirical frequencies in which these transitioning events happen in the sequence. From these empirical frequencies, we built a Markov Chain, as done previously (Demertzi et al. 2019a). More specifically, we counted the number of transitions between all pairs of patterns without considering self-transitions (which correspond to remaining in the same pattern), and normalized these counts to obtain a Markov transition probability matrix $\mathbf{P}$.

Statistical analysis

To assess the statistical significance of comparing different conditions and differences in occurrence rates, slopes' coefficient and Shannon entropy, we performed independent t-test with Bonferonni correction between the awake and anesthesia conditions before any stimulation, and all their associated stimulation conditions, and reported the associated *p* values. We also performed three or two-way ANOVA to confirm that the obtained results of comparing two conditions together (with corrections for multiple comparisons) are consistent with comparing the conditions given the independent variables at play: during/after stimulation, amperage/montage used, and the animal.

All these analyses are shown in table form (Sup. Table 4) following APA standards by reporting the means and standard deviations, the statistics (T-values or F-values), the

degrees of freedom and the *p* values, all to two significant digits. For the ANOVA tests, we also report the sum of squares.

To ensure the reliability of the transition probabilities, we performed a bootstrap method that breaks the temporal dependencies in the chain of visited states. We randomized the order of brain states' appearance, thus conserving the overall statistics, but breaking the temporal dependence between specific pairs of visited states. We performed this randomization 10.000 times and computed as many transition matrices. We asserted that certain states' transitions truly reflected a stochastic process, and were hence not due to chance, by verifying if the empirical transition matrices were above the confidence interval defined by confidence levels of 90%, 95% and 99%. This allows us to somewhat compensate for the animal-specific effects by discarding them. Finally, for the transitions that did pass at least the 90% confidence interval test, we compared, using independent t-tests with Bonferonni correction, the transition probabilities between conditions and reported the associated *p* values.

All these tests were performed using customized codes openly available (https://github.com/Krigsa/phase_coherence_kmeans), using Python libraries such as *add_state_annot* (Charlier et al. 2022), *Scipy* (Virtanen et al. 2020).

RESULTS

We established an experimental procedure that allowed HD-tDCS and fMRI data acquisition in macaque monkeys (Macaca mulatta) under two states of consciousness: awake and general anesthesia (Figure 1). We observed no side effects from the tDCS electrical stimulation, including the absence of erythema at the local sites where the electrodes were placed.

We calculated the dynamic functional connectivity between 82 cortical regions of interest (ROIs), based on a recent anatomical connectivity matrix derived from the CoCoMac

database (Shen et al. 2019; Bakker, Wachtler, and Diesmann 2012). We then used the Hilbert transform to estimate the phase of BOLD signals at each TR, and compute the coordination (based on phase coherences as described in Material & Methods) between the continuous fMRI time series across all ROIs. Subsequently, we applied the unsupervised k-means algorithm to cluster the phase-based coherence matrices. This resulted in the identification of recurrent patterns of brain connectivity. To investigate whether tDCS stimulation alters the relationship between functional and structural connectivities, we finally sorted these brain patterns based on their degree of similarity to the CoCoMac anatomical matrix and calculated relative occurrence rates of the patterns, the structure-function correlation (SFC) and the Shannon entropy for each vigilance state, electrode arrangement and stimulation condition (See Methods, for details).

In the following figures (Figures 1-5), we present the results for brain patterns (or k clusters) fixed to 6, as this number turned out to be the best choice for maximizing the inter-pattern correlation variance (IPCV) when considering awake and anesthesia datasets together (Sup. Figure 1A). Additionally, we verified that varying the number of brain patterns (or k clusters) in the K-means algorithm from 3 to 10 did not change the main results presented below (Sup. Figures 2-4). Boxplots displaying the main measurables (slope's coefficient and Shannon entropy) as a function of said k-number of clusters were also done (Sup. Figures 5-8), hereby showing the consistency of our results regardless of the choice of k. Finally, we also show the full analysis for k=4 for the awake dataset (Sup. Figure 9) and for k=9 for the anesthesia dataset (Sup. Figure 10), as proposed by the IPVC (Sup. Figures 1B&C).

Polarity-dependent effects of prefrontal HD-tDCS on the cortical dynamic connectivity in awake macaque

To examine whether HD-tDCS can perturb the repertoire of functional connectivity patterns characteristic of the awake state, we collected a total of 288 fMRI runs before, during and after the application of HD-tDCS at an intensity of 2 mA in two macaque monkeys, using two different electrode setups (Figure 1A).

The dynamic connectivity analysis was performed on data from all five awake experimental conditions: before HD-tDCS, during HD-tDCS using anodal or cathodal montages and after HD-tDCS (Figure 2). The resulting patterns exhibited various complex configurations of interregional connectivity, ranging from long-range positive/negative coherences (patterns 1 and 3) to mostly frontal positive and parieto-occipital negative coherences (patterns 2 and 4), and to almost strictly positive medium or low interregional coherences (patterns 5 and 6) (Figure 2A). We then calculated the probability distribution of the occurrence of each pattern across the stimulation conditions (Figure 2C). Interestingly, brain pattern 6, referred to as the 'anatomical pattern' due to its highest correlation with the CoCoMac connectome, showed the most numerous and strongest differences in visit frequency. The time spent in this pattern increased sharply both during and following the stimulation with the cathodal montage compared to before the stimulation, as well as compared to the corresponding conditions with the anodal montage, thus demonstrating the specificity of the effect observed. For brain state 5, its time of visit was markedly shorter in the cathodal post-stimulation condition in comparison to before stimulation. Then, cathodal stimulation also shortened the time of visit of brain state 3 during stimulation compared to the corresponding condition with the opposite montage. In sharp contrast, the distribution of occupancies of patterns did not exhibit much change during or following stimulation with the anodal montage, compared to the pre-stimulation. These polarity-specific effects of prefrontal HD-tDCS were further illustrated by plotting the occurrence rate per condition (Figure 2D), which highlighted the substantial increase in brain pattern 6, and the decreases in brain patterns 1, 3, and 5, together with a trend towards increases in patterns 2 and 4 induced by cathodal stimulation, whereas the effects of anodal stimulation were non-significant. These results suggest that the cathodal stimulation lowered the occurrence of patterns with high frontal coherence (patterns 1, 3 and 5), while it promoted the visit of patterns with predominant parieto-occipital coherence (patterns 2 and 4) or very low coherence (pattern 6). All statistics are shown in Sup. Table 4A, including three-way ANOVA tests performed to analyze the effect of tDCS' montage types (anodal and cathodal), tDCS' temporal effects

(during and after stimulation) and individuals on the brain patterns occurrence rates considering interaction terms.

We then computed the Shannon entropy from the normalized histograms of occurrences (Figure 2E, Sup. Table 4A). The Shannon entropy was considerably lower during and after cathodal stimulation compared to before stimulation, and during cathodal stimulation compared to during anodal stimulation. In contrast, the Shannon entropy was not much affected by stimulation with the anodal montage, further supporting the polarity-dependent nature of the effects. This result implies that cathodal, but not anodal stimulation, limits the degree of surprise held in the distribution of pattern rates. Such effects were also characterized and reported in many different studies investigating anesthesia-induced loss of consciousness in humans (Golkowski et al. 2019; Castro et al. 2023), in macaques (Barttfeld et al. 2015; Uhrig et al. 2018); under sleep-induced loss of consciousness in human ((Patel et al. 2020; Castro et al. 2023)) and in patient suffering from disorders of consciousness (Demertzi et al. 2019a). Moreover, it was also shown to be reversible using deep brain stimulation of the central thalamus which restored arousal and wakefulness in macaques (Tasserie et al. 2022; Luppi et al. 2024), as well as upon recovering from general anesthesia (Patel et al. 2020; Castro et al. 2023).

We then evaluated the relationship between the centroids' presence rate and the anatomical backbone in monkeys. For each centroid, we computed its structure-function correlation (SFC), as explained in Material & methods. Thus, we plotted the presence rates of all the centroids, for all macaques, as a function of their SFC (Figures 2F and 2G). Considering the averages of occurrence rates over the different populations, we computed one linear regression (per condition) concerning their associated SFC, corresponding to the overall linear relationship between the time spent in the different brain states, and their similarity to the anatomical connectivity. The corresponding statistics are displayed in Sup. Table 4A. The slope was substantially heightened during and after stimulation with the cathodal montage compared to before stimulation. In addition, during the stimulation, the cathodal montage was associated with a significantly higher slope's coefficient compared to the anodal montage, and similarly when comparing

to the post-stimulation conditions together. Consistent with our previous observations, the stimulation with the anodal montage had a negligible influence on this metric when compared to the pre-stimulation condition. These results weren't affected much by the choice of the number of k clusters (Sup. Figure 5) and similar results were obtained when the full analysis was repeated for k = 4 (Sup. Figure 9), as suggested by the IPVC (Sup. Figure 1B).

Yet, these alterations of brain dynamics were not accompanied by any obvious behavioral change in the monkeys, as evidenced by the fact that they continued to show consistent and optimal eye fixation rates (Sup. Table 2).

Then, we analyzed the succession of brain states through the prism of a Markov chain (as explained in the Material & Methods). We performed pairwise comparisons between the different stimulation conditions and the pre-stimulation condition and confirmed that no effect nor interactions due to the animal were significant. Both anodal and cathodal stimulations produced substantive changes in probability transitions (Figure 3). The corresponding statistics are shown in Sup. Table 4B. Anodal stimulation (montage anodal) significantly influenced transition probabilities, favoring brain state 3 to brain state 5 transitions and reducing brain state 2 to brain state 4 transitions (Figure 3A). Said effects weren't sustained after the stimulation, but still, another perturbation was significantly affected only after the stimulation, from brain states 2 to 6. In summary, anodal PFC HD-tDCS weakly promoted transitions to anatomically similar brain states (brain states 5 and 6).

Interestingly, cathodal stimulation induced much greater transition probabilities towards brain state 6 coming from brain states 1, and 2 (Figure 3B). Conversely, transitions from brain state 2 to 3, from 5 to 2, and from brain state 6 towards brain state 5 were significantly reduced by cathodal stimulation. Other changes were observed only after the cathodal stimulation such as an increase of the probability of transitioning from brain state 5 to 6 and a decrease of the probability of transitioning from brain states 6 to 3. Other transitions were affected both during and after cathodal stimulation, such as the

transitions from brain states 4 and 5 to brain state 6, amongst others, which are favored under and after stimulation but did not pass the bootstrap and/or the ANOVA tests, hence their absence from the figure. To sum up, cathodal PFC HD-tDCS strongly promoted transitions to brain state 6.

Overall, our results show that the Markov chain transition probabilities are affected differently during and after HD-tDCS. Some changes were observed only during ongoing current delivery, while others were specific to the post-stimulation condition when no more current was administered. Importantly, the fact that both categories of changes were found in both cathodal and anodal experiments suggests a general phenomenon.

Contrasting the effects of prefrontal HD-tDCS on the dynamic connectivity patterns in wakeful macaque to unconscious dynamics

As signatures of consciousness lying in brain dynamics have previously been revealed by confronting data from conscious and unconscious states (Barttfeld et al. 2015; Uhrig et al. 2018; Demertzi et al. 2019a; Castro et al. 2023; "Conscious Processing and the Global Neuronal Workspace Hypothesis" 2020), we repeated our analysis to the data from all the five awake experimental conditions merged with the anesthesia pre-stimulation condition (Figure 4). All statistics are shown in Sup. Table 4C. The six resulting brain patterns showed somewhat different trends in terms of connectivity arrangements compared to the patterns that emerged from the analysis of the awake data alone (referred to as 'awake patterns'). While patterns 1 and 2 closely matched awake patterns 1 and 2, the remaining patterns showed distinct connectivity configurations (Figure 4A).

As expected, the awake and the anesthesia pre-stimulation conditions exhibited significant differences in the rates at which the six brain patterns occurred (Figures 4C and 4D). Pattern 1 was present in the awake pre-stimulation condition but virtually absent in the anesthesia pre-stimulation condition, whereas patterns 5 and 6 were preponderant under anesthesia. These findings are consistent with previous dynamic rs-fMRI studies in macaques and humans, showing that wakefulness is typified by the dynamic

exploration of a rich repertoire of functional architectures, whereas under anesthesia the repertoire is mainly constrained by brain anatomy and can present such drastic changes in states' distribution, referred to as diminution of said repertoire (Barttfeld et al. 2015; Uhrig et al. 2018; Demertzi et al. 2019b).

The cathodal montage again produced strong perturbation effects (Figures 4C and 4D). State 4, characterized by short-range frontal coherences, proved to be impacted with a pronounced reduction in its occurrence both during and following the stimulation compared to before stimulation. Then, state 6, the so-called 'anatomical' pattern showed differences between conditions, and consistency regarding the previous analysis (without the anesthesia pre-stimulation condition): cathodal HD-tDCS increased the occurrence rate of said state, and so differently than anodal stimulation. Therefore, consistent with the analysis of awake data taken alone, the reverse stimulation reduced the number of visits of the pattern with a predominant frontal coherence (here pattern 4), while the 'anatomical' pattern (pattern 6) saw an increase in its incidence.

The Shannon entropy was found to be much lower in anesthetized monkeys than in awake animals (Figure 4E), in line with previous studies in humans showing reduced values in states of loss of consciousness, whether related to disorders of consciousness, deep sleep or anesthetic-induced, compared to healthy awake subjects (Demertzi et al. 2019a; Castro et al. 2023). Prefrontal stimulation with the cathodal electrode layout significantly diminished Shannon entropy similarly to the previous uncontrasted analysis, while the anodal montage remained nearly inactive.

A further characterization of how HD-tDCS altered the dynamics of brain coordination was obtained by calculating the slope of SFC with respect to the rate of occurrence of the patterns (Figures 4F and 4G). Consistent with our previous results, the cathodal HD-tDCS induced a direct and lasting effect that was captured in our SFC-frequency analysis, where the states with high SFC were more present compared to those with low SFC. These perturbations were noticeable when considering each individual, as we then looked at the linear regression for every macaque and compared the different conditions'

populations. The effects observed during and after cathodal stimulations were strong enough to alter the slopes. In comparison to the pre-stimulation, the changes observed during and after the stimulation were significant and with similar tendency: an increase in the SFC-slope's coefficient. Finally, these differences were specific to the cathodal montage, as the comparison between the two types of electrode arrangement revealed, again, statistically significant differences. These results, regarding the slope of the linear regression and the Shannon entropy, proved to be robust to the choice of the number of k clusters (Sup. Figure 6).

Effects of prefrontal HD-tDCS on the dynamic connectivity patterns in anesthetized macaque

Under propofol anesthesia, we adopted a slightly different experimental design, aiming to see the increasing effects of anodal HD-tDCS of the PFC with increasing intensity. We acquired fMRI data before, during, and after HD-tDCS delivered at an intensity of 1 mA, followed by a second block of stimulation at 2 mA (Figure 1B). A total of 136 runs were acquired in two macaque monkeys, with anodal stimulation of the left or right PFC, depending on the monkey and its anatomical constraints. We also continuously monitored vital parameters related to hemodynamics, ventilation, and temperature (Sup. Table 3).

The data from the anesthesia experimental conditions were subjected to the dynamic signal coordination analysis: before HD-tDCS, during and following 1 mA HD-tDCS, and during and following 2 mA HD-tDCS (Figure 2). All statistics are shown in Sup. Table 4D.

Compared to the patterns derived from the awake dataset studied alone (Figure 2A), the patterns showed a slightly different organization of interconnectivity between regions, with patterns 2, 3, 4, and 5 displaying primarily frontal/prefrontal coherences (Figure 5A). Interestingly, brain states 2 and 5 presented an increase in their presence rates compared to pre-stimulation, while brain state 6 showed a decrease after 2 mA HD-tDCS (Figure 5C). Effects at the moment of the stimulation were consistent with those after, but not statistically significant compared to pre-stimulation. Plotting the frequency of pattern visits

across conditions further illustrated the notable decrease in the prevalence of brain state 6, the higher occurrence rate of states 2 and 5, as well as a tendency for the effects of the stimulation to gradually rise as a function of stimulation intensity (Figure 5D).

Comparisons of Shannon entropy were non-significant (Figure 5E). However, for the 2 mA post-stimulation condition, the slope coefficient was statistically reduced compared to before stimulation. (Figures 5F and 5G).

Because the IPVC suggested that 9 brain patterns would be optimal to reach the maximum IPVC for the anaesthesia dataset (Sup. Figure 1C), we repeated the full analysis for k=9 (Sup. Figure 10). Using k=9, we found even more perturbations of HD-tDCS of brain dynamics than with k=6: the 'anatomical' brain state's occurrence rate was significantly lower both during and following 2 mA stimulation. Also, the previously labeled brain state 2, which presented an increase in occurrence when stimulated at 2 mA, showed similar results, though this brain state became number 5 (meaning 3 new patterns were found with lower SFC than said state). Then, the reduction in the slope's coefficient due to 2 mA stimulation was also present, though only the post-stimulation condition resulted as statistically significant, and no effect on the Shannon entropy was observed (tendencies still did match).

In a similar approach as to the analysis of the awake dataset, we contrasted the data from all anesthesia conditions with the awake pre-stimulation condition, keeping k=6 for the K-means clustering (Sup. Figure 11). As anticipated, all the patterns except pattern 5 showed significantly different rates of occurrence between the awake and anesthesia pre-stimulation conditions, with pattern 1 being visited in the awake pre-stimulation condition but virtually absent in all the anesthesia conditions, and pattern 6 being more likely to occur in the sedated pre-stimulation condition compared to the awake pre-stimulation condition. These results were consistent with those obtained from the analysis of the awake data contrasted with the anesthesia pre-stimulation condition (Figure 4B). Yet, no change in slope coefficients and Shannon entropy was observed in either stimulation condition compared to anesthesia pre-stimulation, though tendencies were consistent with what was statistically significant without the awake pre-stimulation: during and after

2mA stimulations' population presented lower slope's coefficient and Shannon Entropy, brain state 3 was visited more often than pre-stimulation, and brain state 6 less often.

These results show that 2 mA anodal stimulation of the prefrontal cortex could reconfigure brain dynamics under anesthesia to some extent, but did not reconstitute the full range of characteristics of awake cortical dynamics. Consistent with these findings, these modulations were not accompanied by any behavioral sign of awakening in the animals. Nevertheless, the stimulation did influence some vital parameters (Sup. Table 3). A one-way ANOVA revealed that there was a statistically significant difference in mean heart rate between at least two conditions ($F(4, 111) = [3.64]$, $p = [0.008]$). The Bonferonni test for multiple comparisons found that the mean value of heart rate in the post-stimulation 1 mA and stimulation 2 mA conditions was significantly lower compared to pre-stimulation (($p = 0.024$, 95% C.I. = [0.52,13.05]) and ($p = 0.021$, 95% C.I. = [0.62,13.15]), respectively). There was also a statistically significant difference in mean systolic and diastolic blood pressure between at least two conditions (($F(4, 131) = [2.97]$, $p = [0.022]$) and ($F(4, 130) = [3.07]$, $p = 0.018$]), respectively). The Bonferonni test showed that the mean systolic and diastolic blood pressures for the 2 mA post- stimulation condition were significantly higher compared to the pre-stimulation condition (($p = 0.017$, 95% C.I. = [-13.51,-0.77]) and ($p = 0.033$, 95% C.I. = [-8.36,-0.20]), respectively).

Lastly, we studied how the transitions between brain states changed under stimulated conditions with respect to the anesthesia pre-stimulation, both with and without contrasting with the awake pre-stimulation condition. However, both during and following stimulation, at both 1 and 2 mA, not a single transition passed the bootstrapping method, even with a confidence level of "only" 90%. Thus, we could not interpret any possible changes in transition probability since those empirical transitions can't be considered specific nor temporally independent. As such, we do not show this analysis.

DISCUSSION

The dynamic nature of brain activity and connectivity in resting-state fMRI has attracted considerable interest over the past years. In this study, we demonstrate that tDCS perturbs dynamic brain patterns in awake but also deeply sedated macaques and show that the signatures of consciousness and unconsciousness embedded in cortical brain dynamics can be non-invasively influenced by a weak direct current applied transcranially. Those results are consistent with the hypothesis that tDCS directly affects brain dynamics. In the following, we discuss the implications and potential mechanisms associated with the dynamic changes induced by tDCS.

Cathodal prefrontal HD-tDCS strongly perturbed cortical brain dynamics in awake macaques

In awake animals, our analysis showed that cathodal stimulation of the PFC markedly alters the relative prevalence of cortical signal coordination patterns (Figures 2 and 4). We found that the 'anatomical' pattern (pattern 6) was the most sensitive to the cathodal stimulation. Our observations that the prevalence of this pattern as well as the transitions towards it (Figure 3), are greatly enhanced by the cathodal stimulation in a conscious wakeful context is both unexpected and surprising. One hypothetical explanation might be that this pattern is related to transient drops in vigilance levels and that the cathodal stimulation might enhance such a phenomenon. Contamination of fMRI data by transient periods of microsleep has been shown to occur frequently in awake resting-state experiments (Tagliazucchi and Laufs 2014). Interestingly, some recent papers suggested that tDCS over prefrontal or frontal regions can influence arousal, sleepiness or sleep quality (Annarumma et al., 2018; Krone et al., 2023). For instance, cathodal bi-frontal tDCS delivered immediately before sleep time has been found to increase total sleep time, as well as decrease cortical arousal as measured by resting-state EEG power in healthy volunteers (Frase et al., 2016). However, in our experiments, the stimulated animals did not show any tendency to drowsiness or, on the contrary, any sudden restlessness as a result of trying to resist sleep. Furthermore, the animals were not resting but engaged in a fixation task throughout the fMRI data acquisition. It is also worth noting

that they completed the task with a similar success rate in the cathodal stimulation condition compared to the pre-stimulation or anodal stimulation conditions (Sup. Table 2). This result challenges potential associations with sleepiness or reduction of arousal.

Alternatively, other types of mental processes might be enhanced by cathodal tDCS, such as the tendency to mind-wander, to experience mind-blanking, or to enter a hypnotic state. A seminal study showed that anodal prefrontal cortex stimulation can significantly boost the tendency to mind wander in healthy adults (Axelrod et al. 2015). However, subsequent efforts to replicate these findings yielded conflicting results (see for review (Coulborn and Fernández-Espejo 2022; Kajimura and Nomura 2015; Giacometti Giordani et al. 2023); Nawani et al., 2023). Concerning mind-blanking, in which the mind is alert but is not actively engaged in a specific cognitive task, reports of mind-blanking were recently found to correlate with a pattern of global positive-phase coherence, rather than the pattern that most closely resembles anatomy (Mortaheb et al. 2022).

Finally, cathodal left DLPFC tDCS was demonstrated to enhance hypnotizability by 15% and to alter some dimensions of consciousness, significantly increasing attention, absorption and time sense while decreasing self-awareness and memory (Rinaldo L. Perri et al. 2022; Rinaldo Livio Perri and Di Filippo 2023). While our observations of the monkey's high fixation task performance would be consistent with increased attention or absorption, the demonstration of a modulatory effect of cathodal tDCS on one or other of these specific mental processes or dimensions of consciousness will require further investigations in humans using relevant behavioral measures, cognitive tasks and brain activity tracking.

Anodal prefrontal HD-tDCS perturbed cortical brain dynamics, especially during deep anesthesia.

In awake macaques, we found that the anodal montage significantly disturbed some of the transition probabilities between the brain states (Figure 3), tended to decrease the slope's coefficient (Figure 4F,G) and increase the occurrence rate of brain state 1 (Figures 2C,D, 4C,D). Although small, these changes would be compatible with recent

literature suggesting that anodal PFC tDCS, when delivered during the daytime, can positively influence levels of vigilance and sleepiness (Annarumma et al. 2018). For example, this type of stimulation has been described to increase beta and decrease delta powers in a wakeful context, suggestive of an enhanced vigilance (Keeser et al. 2011; Wirth et al. 2011; Maeoka et al. 2012; Dai et al. 2022). Bifrontal anodal stimulation was found to increase objective and subjective vigilance and reduce daytime sleepiness in a patient with organic hyperinsomnia following reanimation (Frase et al., 2015). Moreover, in sleep-deprived adults, it also reduces EEG correlates of physiological sleepiness (Alfonsi et al. 2023). Anodal left DLPFC tDCS performed better than caffeine in preventing the reduction in vigilance and alleviating subjective ratings of fatigue and drowsiness in sleep-deprived individuals (McIntire et al. 2014). Finally, such a stimulation also affected total sleep time, shortening it by about 25 min, when administered just before sleep in healthy volunteers (Frase et al. 2016).

While we observed modest effects of anodal PFC HD-tDCS in awake animals, the stimulation induced significant changes in cortical brain dynamics under anesthesia (Figure 5 and Sup. Figure 10), which globally resisted contrasting with the awake pre-stimulation condition (Sup. Figure 11). This finding suggested that 2 mA anodal HD-tDCS could positively influence the signatures of consciousness under anesthesia (Barttfeld et al. 2015; Uhrig et al. 2018; Demertzi et al. 2019a; Castro et al. 2023). It's also important to mention that the 2 mA stimulation reduced the SFC frequency slope to a value somewhat in between the anaesthesia and awake pre-stimulation conditions (Sup. Figure 11F,G). Therefore, although our protocol did not succeed in awakening the sedated animals, our results support the ability of prefrontal tDCS to affect markers of consciousness in the context of an anesthetized-induced loss of consciousness. It can be hypothesized that there was a stronger molecular effect of the anesthetic drug than an electrical effect at an intensity of 2 mA, which could explain the lack of behavioural effects. It remains however possible that a similar protocol could succeed in awakening macaques sedated with a lower dose of propofol or in reversing unconsciousness due to deep propofol anesthesia with stronger stimulation intensity. In this case, the effects may reach a (hypothetical) threshold where we get as much disturbance from pharmacology

as physical intervention, thus resulting in an observable behavioral effect of tDCS (suggested by the fact that we observed a greater effect on brain dynamics at 2 mA compared to 1 mA).

Interestingly, recent research in humans showed that tDCS delivered at 4 mA intensity can robustly enhance the effects of the stimulation compared to 2 mA and is safe, well-tolerated and without adverse effects (e.g., (Michael A. Nitsche and Bikson 2017; Roncero et al. 2021; Hsu et al. 2023). Therefore, our results encourage further investigation using anodal prefrontal HD-tDCS at an intensity of 4 mA to non-invasively attempt to reverse the effects of deep propofol anaesthesia. Our findings also provide support for the use of tDCS to promote rapid recovery from general anesthesia in humans (Kato and Solt 2021) and suggest that a single anodal prefrontal stimulation at the end of the anesthesia protocol may prove to be effective for this purpose.

From another clinical perspective, our results showing that 2 mA anodal PFC tDCS can positively influence the dynamic signatures of consciousness during anesthesia, are also consistent with the beneficial effects of such stimulation reported in DOCs patients (e.g., (Thibaut et al. 2014; Angelakis et al. 2014)). For instance, recent meta-analyses have concluded that tDCS is more effective in improving the level of consciousness in patients with a minimally conscious state (MCS) than in those with an unresponsive wakefulness syndrome (UWS), which is a more severe form of this medical condition (Xu et al. 2022; Liu et al. 2023). Our results support the efficacy of tDCS in improving consciousness markers in patients with DOCs, particularly in the least severely affected patients, and encourage the design of new clinical trials to investigate the effects of higher stimulation intensities.

From a mechanistic point of view, prefrontal tDCS may modulate arousal and improve the level of consciousness by acting on the recently proposed cortico-thalamic pathway of sleep-wake regulation or by acting directly on the ascending thalamocortical pathway, which originates in the brainstem (for review, see (Krone et al. 2017)). Depending on electrode positions and the stimulation parameters, tDCS has been shown to directly

modulate subcortical regions. For example, fronto-temporal tDCS has been reported to alter corticostriatal and corticothalamic rs-fMRI connectivity in healthy volunteers (Krone et al. 2017; Polanía, Paulus, and Nitsche 2012; Dalong et al. 2020). In vivo measurements in humans using intracerebral electrodes confirmed that the stimulation can generate a biologically relevant electric field at the subthalamic level or other deep brain structures (for review see (Guidetti et al. 2022; Louviot et al. 2022)). A future computational investigation of the electric field generated by the specific fronto-occipital montage utilized in this study will likely yield valuable information regarding which pathway, cortico-thalamic or thalamocortical, may have been modulated here (Saturnino et al. 2019; Y. Huang et al. 2012). Furthermore, modulation of intrinsic networks (Raichle et al. 2001; Boly et al. 2008) is possible in light of our result and could also be investigated with the means of iCAPs-based analysis (Karahanoğlu and Van De Ville 2015).

From a biophysical standpoint, Bikson and his colleagues have provided evidence that anodal stimulation leads to depolarization at the soma of neurons in rat hippocampal slices, while cathodal stimulation induces their hyperpolarization, especially when the current is aligned with the soma-apical axis (Bikson et al. 2004). These findings were corroborated in human subjects (M. A. Nitsche and Paulus 2000), where anodal tDCS applied to the motor cortex increased the amplitude of motor evoked potentials in response to transcranial magnetic stimulation, while cathodal M1 stimulation had the opposite effects, revealing an increase or decrease in M1 excitability, respectively. The magnitude of these effects was small (0.2 mV) (Bikson et al. 2004) but fell within the range of endogenous electric field interactions generated between cortical columns, where it can be greatly amplified by recurrent interactions (Rebollo et al. 2021). Interestingly, in the awake state, we observed that cathodal stimulation of the PFC induced a significant decrease in the frequencies of patterns exhibiting high frontal coherence (patterns 2 and 5), which is consistent with a decrease in PFC excitability under the cathodal electrode. In contrast, the stimulation tended to increase the frequency of patterns with a predominant parieto-occipital coherence (patterns 2 and 4), which is in line with an increase in excitability under the anodal electrode positioned over the occipital cortex (Figure 2A and C). Under anesthesia, 2 mA anodal HD-tDCS of the PFC increased the

frequencies of patterns exhibiting a high frontal coherence (patterns 2 and 5) (Figure 5A and C), also supporting enhanced excitability under the anodal electrode in deep sedation. It is important to note that the effects of the neuromodulatory ascending systems on brain activation are known to be mediated both by neuronal depolarization and by inhibition of voltage and calcium-dependent conductances, responsible for spike-frequency adaptation in pyramidal cells (Steriade and McCarley 2013; McCormick 1992). Therefore, one possible explanation for the inability of anodal stimulation of the PFC to arouse macaques from anesthesia is that it induced only a partial brain activation, causing depolarization of neurons without affecting spike-frequency adaptation.

Markov chain analysis revealed differential HD-tDCS effects on transition probabilities during and after stimulation

Our results showed relatively similar effects in terms of brain pattern occurrence rates, Shannon entropy and SFC during and after the stimulation (Figures 2, 4 and 5, Sup. Figures 9-11). In contrast, Markov chain analysis revealed the existence of specific transition probability changes induced by HD-tDCS, some of which were found only during stimulation and others exclusively in the post-stimulation condition (Figures 3, Sup. Table 4B). The characterization of the effects elicited during versus following the stimulation is a matter of interest, as it may provide valuable information about the mechanisms of action of tDCS, which are still poorly understood (Lefaucheur et al. 2017). Our results highlight that the specificity of certain effects of HD-tDCS on brain dynamics relative to the time course of the stimulation can hence be revealed using particular dynamic analyses such as the Markov chain transition.

Limitations

One limitation of our study is that we only presented anodal stimulation of the PFC in anesthesia experiments, without cathodal PFC stimulation. Additionally, we did not show a sham control condition to achieve adequate blinding in parallel with the 'active' conditions in the awake and anesthetized experiments. However, the relevance of a sham condition during anesthesia is questionable and concerns have recently been raised

about the neurobiological inertia of certain sham protocols (Fonteneau et al. 2019). Besides, the analytic methodology used in our study is also to nuance: while we do find centroids corresponding to stereotypical brain states of synchronizations and anti-synchronizations between different brain areas, we don't quantify how far we are at each TR from these centroids. Quantifying how well/poorly this methodology performs as a function of frequency components of a signal remains yet to be quantified in a future study as it requires thorough analyses with proper controls and non-linear signals (potentially appearing in empirical data).

Conclusion

We tested the feasibility of perturbing fMRI brain dynamics across states of consciousness using non-invasive neuromodulation in non-human primates. Our results provide the first experimental evidence that HD-tDCS of the prefrontal cortex modulates spontaneous brain activity whether the animals are wakeful and conscious, or unconscious under general anesthesia. This study offers a deeper understanding of how tDCS influences and alters brain dynamics, which is crucial given the growing applications and benefits of this technique in neuroscience and the management of various neurological conditions. Finally, our work suggests that tDCS may be a valuable tool for further exploring the relationship between brain dynamics and states of consciousness, conscious processing, or vigilance by allowing a soft, non-invasive and reversible perturbation of brain activity.

Figure legends.

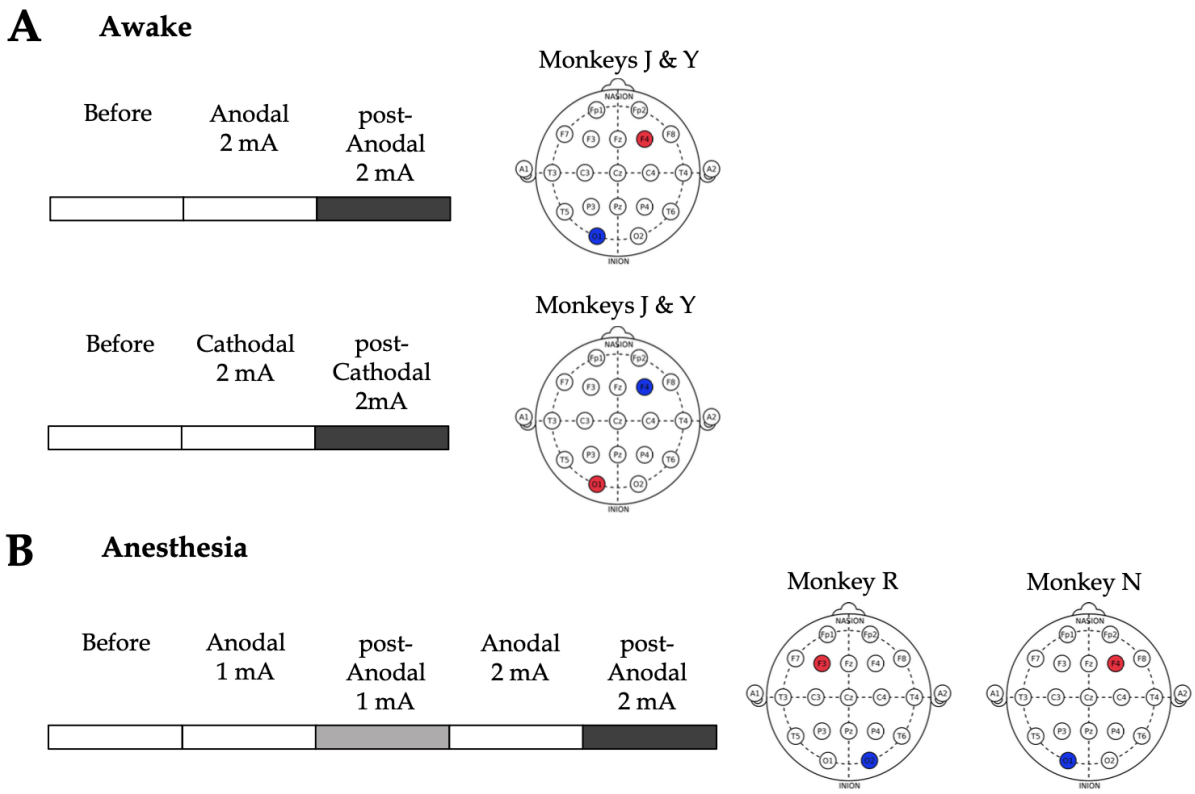

Figure 1. Schematic representation of the experimental designs and HD-tDCS electrode montages employed in the study.

A) Awake experiments. fMRI data were acquired before, during and after a tDCS stimulation of 2 mA intensity. The anodal electrode (red) was either placed over the right prefrontal cortex (F4) and the cathodal electrode (blue) over the left occipital cortex (O1) (anodal montage; top), or a “reversed” montage was used, with the cathodal electrode over F4 and the anodal electrode over O1 (cathodal montage; bottom). B) Anesthesia experiments. fMRI data were recorded before, during and after successive 1 mA and 2 mA tDCS stimulations. An anodal electrode montage was employed, targeting left or right prefrontal cortex (F4/O1 or F3/O2) depending on the animal and its anatomical constraints. Before: before stimulation. Anodal and post-Anodal: during and after anodal HD-tDCS of the PFC. Cathodal and post-Cathodal: during and after cathodal HD-tDCS of the PFC.

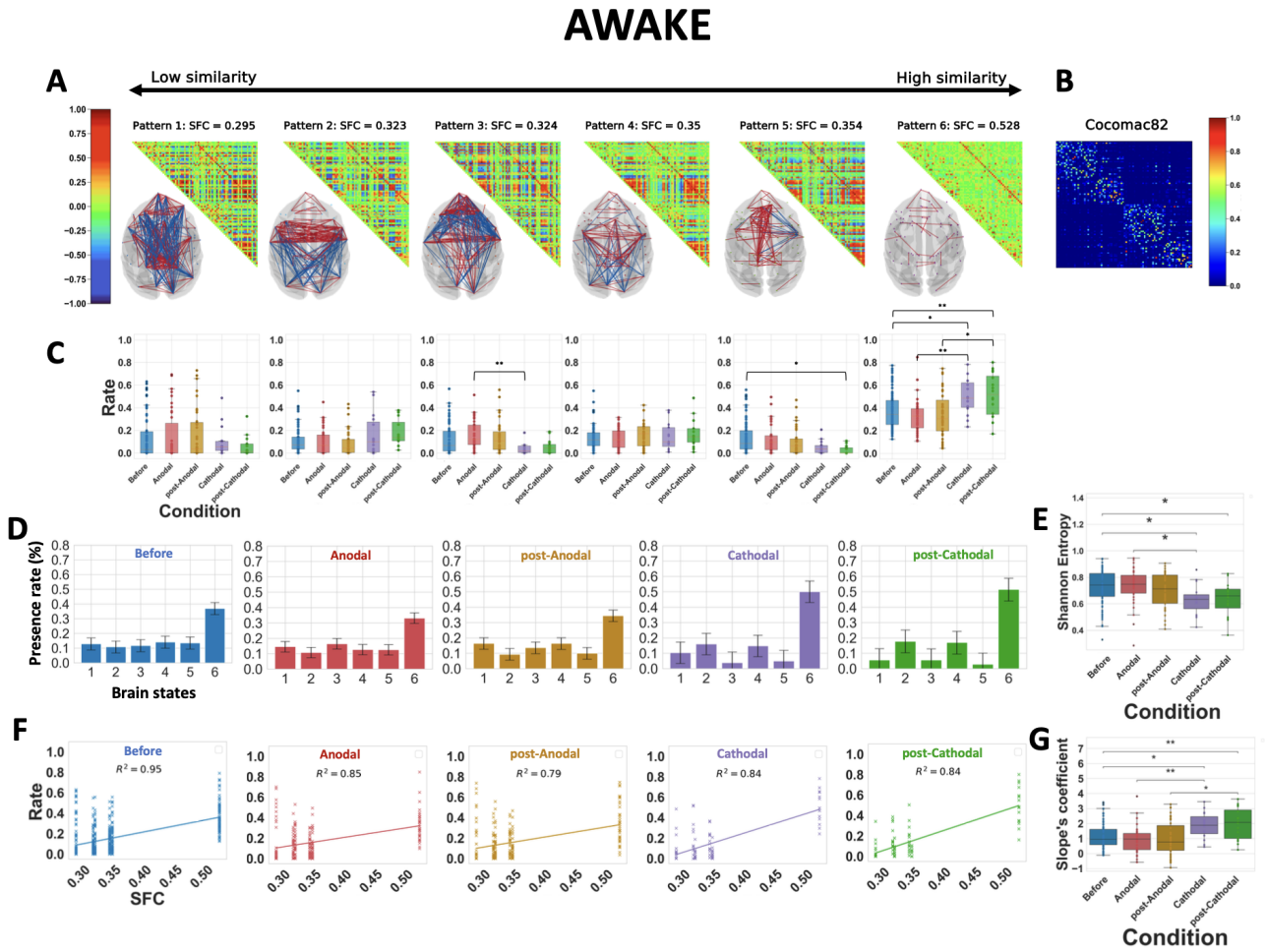

Figure 2. Cathodal but not anodal HD-tDCS of the prefrontal cortex alters the repertoire of functional brain patterns, increases structure-function coupling and decreases Shannon Entropy in awake animals.

A) Matrix representation of the brain patterns for k = 6, obtained by including all the five awake conditions. Brain coordination patterns are ranked from least (left) to highest (right) correlation to the structural connectivity matrix. Networks are plotted in anatomical space (transverse view), showing only the values <-0.5 and >0.5. Red lines represent positive synchronizations between regions of interest, and blue lines represent negative ones. B) Macaque connectome in the CoCoMac82 parcellation. C) Rate of occurrence of each brain connectivity pattern across the five conditions. Boxplots show median occurrence rates with interquartile range, and maximum-minimum values (whiskers). D) Barplots of the 6 brain states and their average presence rate over the population of the different conditions. E) Normalized Shannon Entropy as a function of the conditions. F) Rates of

occurrence of brain patterns as a function of their similarity in functional and structural connectivity (SFC) for the five conditions. Lines are calculated, per conditions, based on the best linear fit between the population's average presence rate of each pattern and their SFC; R^2, Spearman correlation. Crosses represent individuals' presence rates. G) Coefficient of the linearly regressed slope across conditions. Before: before stimulation. Anodal and post-Anodal: during and after anodal HD-tDCS of the PFC (F4/O1 montage). Cathodal and post-Cathodal: during and after cathodal HD-tDCS of the PFC (O1/F4 montage).

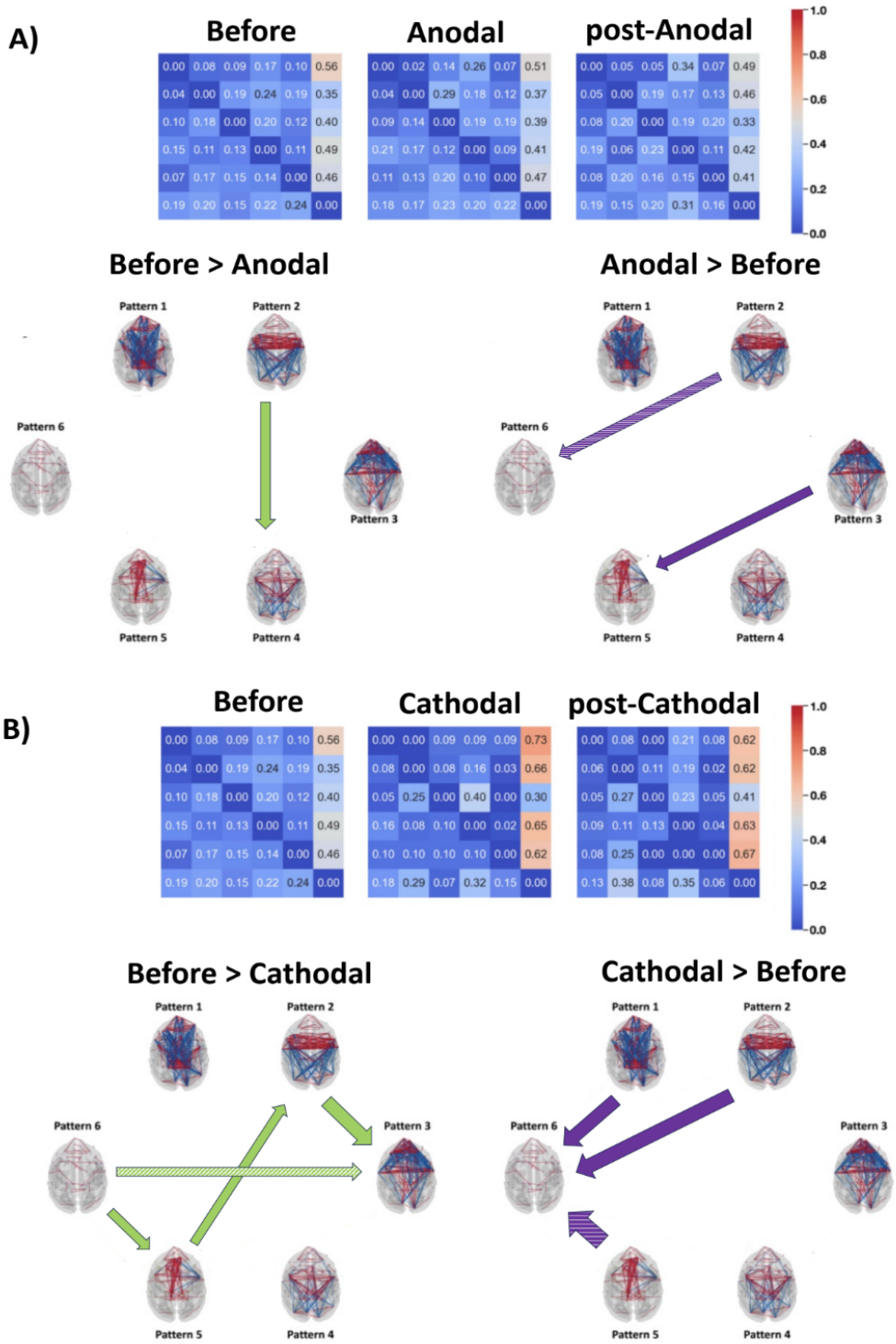

Figure 3. Transition probabilities and Markov chain analysis of the identified brain states during and after anodal or cathodal PFC stimulation in the awake state.

A) Top panels: overall transition probabilities matrices for the pre-stimulation (Before), during stimulation (Anodal) and post-stimulation (post-Anodal) conditions. Lower left

panel: transition probabilities greater before stimulation than during stimulation (full green arrows) or post-stimulation (hashed green arrows). Lower right panel: transition probabilities greater during (full purple arrows) or after (hashed purple arrows) the stimulation than before. B) Top panels: overall transition probabilities matrices for the pre-stimulation (Before), during stimulation (Cathodal) and post-stimulation (post-Cathodal) conditions. Lower left panel: transition probabilities greater before stimulation than during stimulation (full green arrows) or post-stimulation (hashed green arrows). Lower right panel: transition probabilities greater during (full purple arrows) or after (hashed purple arrows) the stimulation than before. Arrow size indicates *p* value significance.

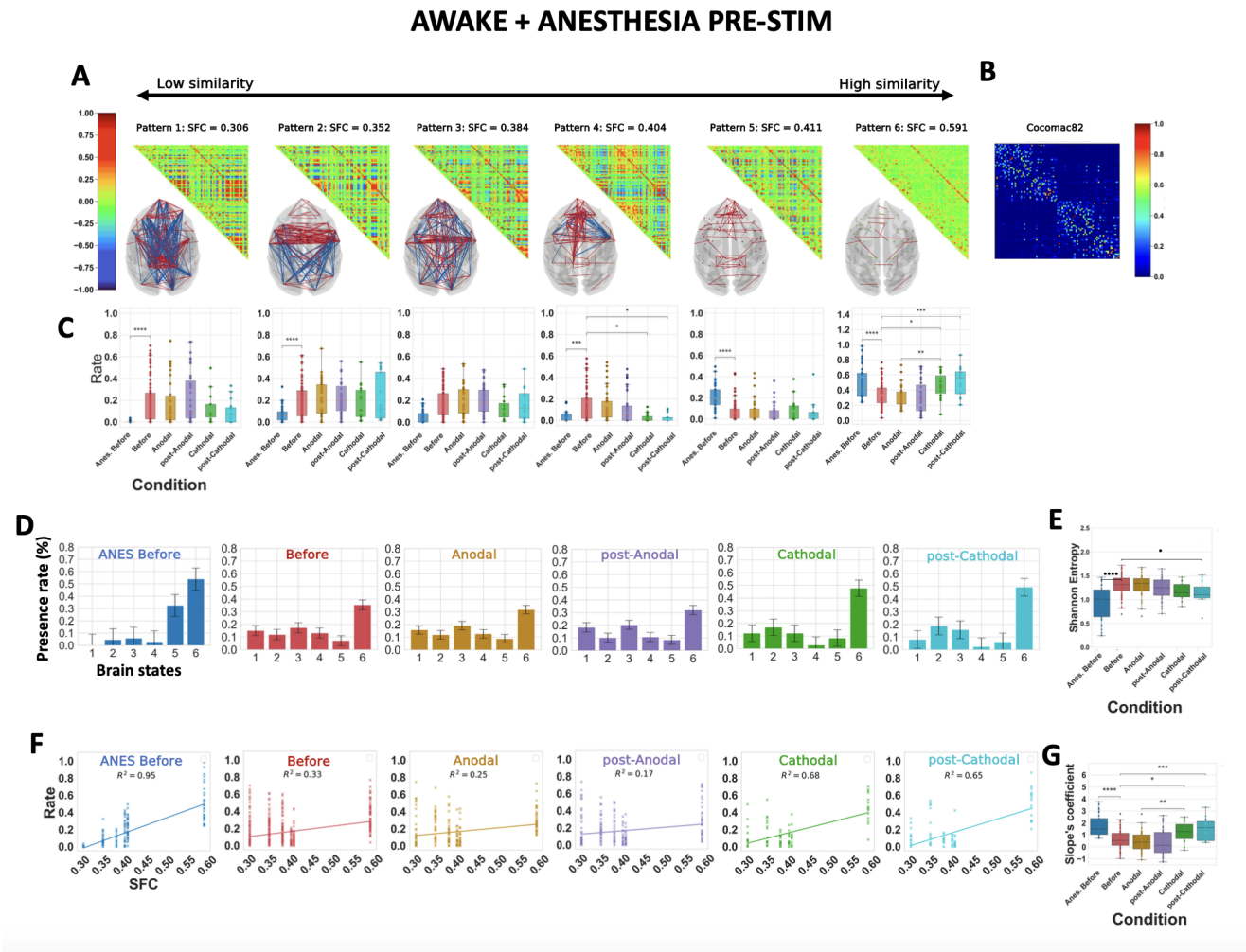

Figure 4. The polarity-dependent effects of prefrontal HD-tDCS on awake brain dynamics resist contrasting with anesthetized dynamics.

Similar analysis than in Figure 2 for k=6 considering all the 5 awake conditions plus the anesthesia pre-stimulation condition. Anes. Before: before stimulation under anesthesia. Before: before stimulation in the awake state. Anodal and post-Anodal: during and after anodal HD-tDCS of the PFC (F4/O1 montage) in the awake state. Cathodal and post-Cathodal: during and after cathodal HD-tDCS of the PFC (O1/F4 montage) in the awake state.

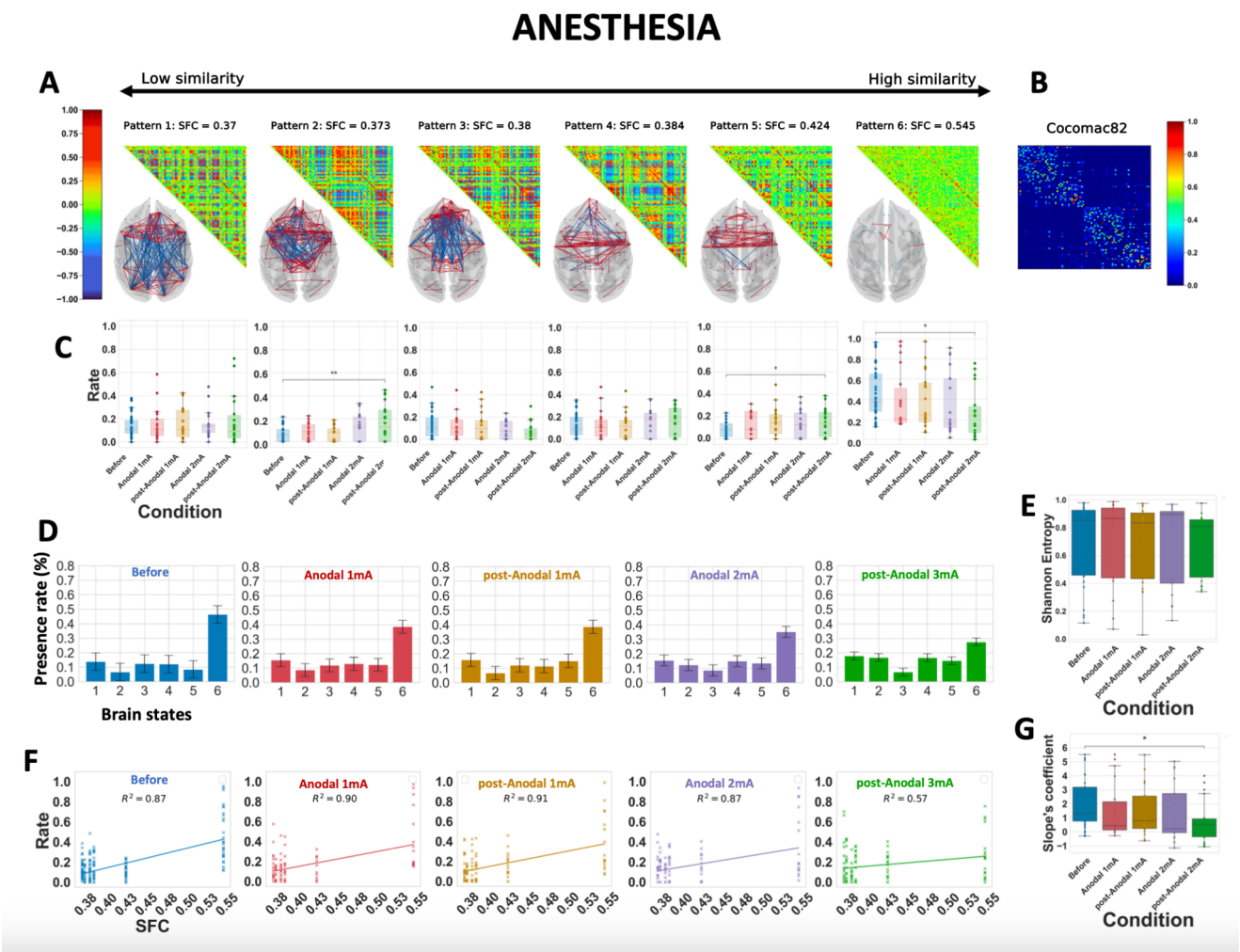

Figure 5. Anodal 2 mA HD-tDCS applied to the prefrontal cortex modifies cortical brain dynamics, reducing structure-function coupling, but does not influence Shannon entropy in anesthetized animals.

Similar analysis than in Figures 2 & 3 for k=6 considering all the 5 anesthesia conditions. Before: before stimulation. Anodal 1 mA and post-Anodal 1 mA: during and after anodal HD-tDCS of the PFC (F4/O1 or F3/O2) delivered at an intensity of 1 mA. Anodal 2 mA and post-Anodal 2 mA: during and after anodal HD-tDCS of the PFC (F4/O1 or F3/O2 montage) delivered at an intensity of 2 mA.

REFERENCES

Alfonsi, Valentina, Aurora D'Atri, Serena Scarpelli, Maurizio Gorgoni, Francesco Giacinti, Ludovica Annarumma, Federico Salfi, Giulia Amicucci, Domenico Corigliano, and Luigi De Gennaro. 2023. "The Effects of Bifrontal Anodal Transcranial Direct Current Stimulation (tDCS) on Sleepiness and Vigilance in Partially Sleep-Deprived Subjects: A Multidimensional Study." *Journal of Sleep Research* 32 (4): e13869.

Allen, Elena A., Eswar Damaraju, Sergey M. Plis, Erik B. Erhardt, Tom Eichele, and Vince D. Calhoun. 2014. "Tracking Whole-Brain Connectivity Dynamics in the Resting State." *Cerebral Cortex* 24 (3): 663–76.

Alonso Martínez, Sonsoles, Gustavo Deco, Gert J. Ter Horst, and Joana Cabral. 2020. "The Dynamics of Functional Brain Networks Associated With Depressive Symptoms in a Nonclinical Sample." *Frontiers in Neural Circuits* 14 (September): 570583.

Angelakis, Efthymios, Evangelia Liouta, Nikos Andreadis, Stephanos Korfias, Periklis Ktonas, George Stranjalis, and Damianos E. Sakas. 2014. "Transcranial Direct Current Stimulation Effects in Disorders of Consciousness." *Archives of Physical Medicine and Rehabilitation* 95 (2): 283–89.

Annarumma, Ludovica, Aurora D'Atri, Valentina Alfonsi, and Luigi De Gennaro. 2018. "The Efficacy of Transcranial Current Stimulation Techniques to Modulate Resting-State EEG, to Affect Vigilance and to Promote Sleepiness." *Brain Sciences* 8 (7). https://doi.org/10.3390/brainsci8070137.

Antonenko, Daria, Anna Elisabeth Fromm, Friederike Thams, Ulrike Grittner, Marcus Meinzer, and Agnes Flöel. 2023. "Microstructural and Functional Plasticity Following Repeated Brain Stimulation during Cognitive Training in Older Adults." *Nature Communications* 14 (1): 3184.

Axelrod, Vadim, Geraint Rees, Michal Lavidor, and Moshe Bar. 2015. "Increasing Propensity to Mind-Wander with Transcranial Direct Current Stimulation." *Proceedings of the National Academy of Sciences of the United States of America* 112 (11): 3314–19.

Baker, Adam P., Matthew J. Brookes, Iead A. Rezek, Stephen M. Smith, Timothy Behrens, Penny J. Probert Smith, and Mark Woolrich. 2014. "Fast Transient Networks in Spontaneous Human Brain Activity." *eLife* 3 (March): e01867.

Bakker, Rembrandt, Thomas Wachtler, and Markus Diesmann. 2012. "CoCoMac 2.0 and the Future of Tract-Tracing Databases." *Frontiers in Neuroinformatics* 6 (December): 30.

Barbati, Saviana Antonella, Maria Vittoria Podda, and Claudio Grassi. 2022. "Tuning Brain Networks: The Emerging Role of Transcranial Direct Current Stimulation on Structural Plasticity." *Frontiers in Cellular Neuroscience* 16 (July): 945777.

Barttfeld, Pablo, Lynn Uhrig, Jacobo D. Sitt, Mariano Sigman, Béchir Jarraya, and Stanislas Dehaene. 2015. "Signature of Consciousness in the Dynamics of Resting-State Brain Activity." *Proceedings of the National Academy of Sciences of the United States of America* 112 (3): 887–92.

Bikson, Marom, Masashi Inoue, Hiroki Akiyama, Jackie K. Deans, John E. Fox,

Hiroyoshi Miyakawa, and John G. R. Jefferys. 2004. “Effects of Uniform Extracellular DC Electric Fields on Excitability in Rat Hippocampal Slices in Vitro.” *The Journal of Physiology* 557 (Pt 1): 175–90.

Biswal, Bharat B. 2012. “Resting State fMRI: A Personal History.” *NeuroImage* 62 (2): 938–44.

Biswal, B., F. Z. Yetkin, V. M. Haughton, and J. S. Hyde. 1995. “Functional Connectivity in the Motor Cortex of Resting Human Brain Using Echo-Planar MRI.” *Magnetic Resonance in Medicine: Official Journal of the Society of Magnetic Resonance in Medicine / Society of Magnetic Resonance in Medicine* 34 (4): 537–41.

Boly, M., C. Phillips, L. Tshibanda, A. Vanhaudenhuyse, M. Schabus, T. T. Dang-Vu, G. Moonen, R. Hustinx, P. Maquet, and S. Laureys. 2008. “Intrinsic Brain Activity in Altered States of Consciousness: How Conscious Is the Default Mode of Brain Function?” *Annals of the New York Academy of Sciences* 1129: 119–29.

Bouchard, Amy E., Emmanuelle Renauld, and Shirley Fecteau. 2023. “Changes in Resting-State Functional MRI Connectivity during and after Transcranial Direct Current Stimulation in Healthy Adults.” *Frontiers in Human Neuroscience* 17 (July): 1229618.

Bracewell, Ronald Newbold. 2000. *The Fourier Transform and Its Applications*. McGraw Hill.

Cabral, Joana, Diego Vidaurre, Paulo Marques, Ricardo Magalhães, Pedro Silva Moreira, José Miguel Soares, Gustavo Deco, Nuno Sousa, and Morten L. Kringelbach. 2017. “Cognitive Performance in Healthy Older Adults Relates to Spontaneous Switching between States of Functional Connectivity during Rest.” *Scientific Reports* 7 (1): 5135.

Calhoun, Vince D., Robyn Miller, Godfrey Pearlson, and Tulay Adalı. 2014. “The Chronnectome: Time-Varying Connectivity Networks as the next Frontier in fMRI Data Discovery.” *Neuron* 84 (2): 262–74.

Castro, Pablo, Andrea Luppi, Enzo Tagliazucchi, Yonatan S-Perl, Lorina Naci, Adrian M. Owen, Jacobo D. Sitt, Alain Destexhe, and Rodrigo Cofré. 2023. “Dynamical Structure-Function Correlations Provide Robust and Generalizable Signatures of Consciousness in Humans.” *bioRxiv*. https://doi.org/10.1101/2023.12.19.572402.

Cavinato, Marianna, Clara Genna, Emanuela Formaggio, Caterina Gregorio, Silvia F. Storti, Paolo Manganotti, Emanuela Casanova, Roberto Piperno, and Francesco Piccione. 2019. “Behavioural and Electrophysiological Effects of tDCS to Prefrontal Cortex in Patients with Disorders of Consciousness.” *Clinical Neurophysiology: Official Journal of the International Federation of Clinical Neurophysiology* 130 (2): 231–38.

Chan, Melody My, and Yvonne My Han. 2020. “The Effect of Transcranial Direct Current Stimulation in Changing Resting-State Functional Connectivity in Patients With Neurological Disorders: A Systematic Review.” *Journal of Central Nervous System Disease* 12 (December): 1179573520976832.

Charlier, Florian, Marc Weber, Dariusz Izak, Emerson Harkin, Marcin Magnus, Joseph Lalli, Louison Fresnais, et al. 2022. *Trevismd/statannotations: v0.5*. Zenodo. https://doi.org/10.5281/ZENODO.7213391.

Cirillo, G., G. Di Pino, F. Capone, F. Ranieri, L. Florio, V. Todisco, G. Tedeschi, K. Funke, and V. Di Lazzaro. 2017. “Neurobiological after-Effects of Non-Invasive

Brain Stimulation." *Brain Stimulation* 10 (1): 1–18.
"Conscious Processing and the Global Neuronal Workspace Hypothesis." 2020. *Neuron* 105 (5): 776–98.
Cornblath, Eli J., Arian Ashourvan, Jason Z. Kim, Richard F. Betzel, Rastko Ciric, Azeez Adebimpe, Graham L. Baum, et al. 2020. "Temporal Sequences of Brain Activity at Rest Are Constrained by White Matter Structure and Modulated by Cognitive Demands." *Communications Biology* 3 (1): 261.
Coulborn, Sean, and Davinia Fernández-Espejo. 2022. "Prefrontal tDCS Is Unable to Modulate Mind Wandering Propensity or Underlying Functional or Effective Brain Connectivity." *Scientific Reports* 12 (1): 18021.
Dai, Jing, Hang Wang, Lin Yang, Chunchen Wang, Shan Cheng, Taihui Zhang, Jin Ma, Zhihong Wen, Xinsheng Cao, and Wendong Hu. 2022. "The Neuroelectrophysiological and Behavioral Effects of Transcranial Direct Current Stimulation on Executive Vigilance under a Continuous Monotonous Condition." *Frontiers in Neuroscience* 16 (September): 910457.
Dalong, Guo, Li Jiyuan, Zhang Ying, Zha Lei, Hou Yanhong, and Shao Yongcong. 2020. "Transcranial Direct Current Stimulation Reconstructs Diminished Thalamocortical Connectivity during Prolonged Resting Wakefulness: A Resting-State fMRI Pilot Study." *Brain Imaging and Behavior* 14 (1): 278–88.
Damoiseaux, J. S., S. A. R. B. Rombouts, F. Barkhof, P. Scheltens, C. J. Stam, S. M. Smith, and C. F. Beckmann. 2006. "Consistent Resting-State Networks across Healthy Subjects." *Proceedings of the National Academy of Sciences of the United States of America* 103 (37): 13848–53.
Datta, Abhishek, Varun Bansal, Julian Diaz, Jinal Patel, Davide Reato, and Marom Bikson. 2009. "Gyri-Precise Head Model of Transcranial Direct Current Stimulation: Improved Spatial Focality Using a Ring Electrode versus Conventional Rectangular Pad." *Brain Stimulation* 2 (4): 201–7, 207.e1.
Deco, Gustavo, Viktor K. Jirsa, and Anthony R. McIntosh. 2011. "Emerging Concepts for the Dynamical Organization of Resting-State Activity in the Brain." *Nature Reviews. Neuroscience* 12 (1): 43–56.
———. 2013. "Resting Brains Never Rest: Computational Insights into Potential Cognitive Architectures." *Trends in Neurosciences* 36 (5): 268–74.
De Luca, Marilena, Stephen Smith, Nicola De Stefano, Antonio Federico, and Paul M. Matthews. 2005. "Blood Oxygenation Level Dependent Contrast Resting State Networks Are Relevant to Functional Activity in the Neocortical Sensorimotor System." *Experimental Brain Research. Experimentelle Hirnforschung. Experimentation Cerebrale* 167 (4): 587–94.
Demertzi, A., E. Tagliazucchi, S. Dehaene, G. Deco, P. Barttfeld, F. Raimondo, C. Martial, et al. 2019a. "Human Consciousness Is Supported by Dynamic Complex Patterns of Brain Signal Coordination." *Science Advances* 5 (2): eaat7603.
———. 2019b. "Human Consciousness Is Supported by Dynamic Complex Patterns of Brain Signal Coordination." *Science Advances* 5 (2): eaat7603.
Dmochowski, Jacek P., Abhishek Datta, Marom Bikson, Yuzhuo Su, and Lucas C. Parra. 2011. "Optimized Multi-Electrode Stimulation Increases Focality and Intensity at Target." *Journal of Neural Engineering* 8 (4): 046011.
Fonteneau, Clara, Marine Mondino, Martijn Arns, Chris Baeken, Marom Bikson, Andre

R. Brunoni, Matthew J. Burke, et al. 2019. “Sham tDCS: A Hidden Source of Variability? Reflections for Further Blinded, Controlled Trials.” *Brain Stimulation* 12 (3): 668–73.

Fox, Michael D., Maurizio Corbetta, Abraham Z. Snyder, Justin L. Vincent, and Marcus E. Raichle. 2006. “Spontaneous Neuronal Activity Distinguishes Human Dorsal and Ventral Attention Systems.” *Proceedings of the National Academy of Sciences of the United States of America* 103 (26): 10046–51.

Frase, Lukas, Hannah Piosczyk, Sulamith Zittel, Friederike Jahn, Peter Selhausen, Lukas Krone, Bernd Feige, et al. 2016. “Modulation of Total Sleep Time by Transcranial Direct Current Stimulation (tDCS).” *Neuropsychopharmacology: Official Publication of the American College of Neuropsychopharmacology* 41 (10): 2577–86.

Frey, Stephen, Deepak N. Pandya, M. Mallar Chakravarty, Lara Bailey, Michael Petrides, and D. Louis Collins. 2011. “An MRI Based Average Macaque Monkey Stereotaxic Atlas and Space (MNI Monkey Space).” *NeuroImage* 55 (4): 1435–42.

Gbadeyan, Oyetunde, Katie McMahon, Marco Steinhauser, and Marcus Meinzer. 2016. “Stimulation of Dorsolateral Prefrontal Cortex Enhances Adaptive Cognitive Control: A High-Definition Transcranial Direct Current Stimulation Study.” *The Journal of Neuroscience: The Official Journal of the Society for Neuroscience* 36 (50): 12530–36.

Giacometti Giordani, Luca, Andrea Crisafulli, Giovanni Cantarella, Alessio Avenanti, and Elisa Ciaramelli. 2023. “The Role of Posterior Parietal Cortex and Medial Prefrontal Cortex in Distraction and Mind-Wandering.” *Neuropsychologia* 188 (September): 108639.

Glerean, Enrico, Juha Salmi, Juha M. Lahnakoski, Iiro P. Jääskeläinen, and Mikko Sams. 2012. “Functional Magnetic Resonance Imaging Phase Synchronization as a Measure of Dynamic Functional Connectivity.” *Brain Connectivity* 2 (2): 91–101.

Golkowski, Daniel, Stephen Karl Larroque, Audrey Vanhaudenhuyse, Alain Plenevaux, Melanie Boly, Carol Di Perri, Andreas Ranft, et al. 2019. “Changes in Whole Brain Dynamics and Connectivity Patterns during Sevoflurane- and Propofol-Induced Unconsciousness Identified by Functional Magnetic Resonance Imaging.” *Anesthesiology* 130 (6): 898–911.

Guidetti, Matteo, Mattia Arlotti, Tommaso Bocci, Anna Maria Bianchi, Marta Parazzini, Roberta Ferrucci, and Alberto Priori. 2022. “Electric Fields Induced in the Brain by Transcranial Electric Stimulation: A Review of In Vivo Recordings.” *Biomedicines* 10 (10). https://doi.org/10.3390/biomedicines10102333.

Guo, Yongkun, Yang Bai, Xiaoyu Xia, Jinju Li, Xiaoli Wang, Yiwu Dai, Yuanyuan Dang, Jianghong He, Chunying Liu, and Hui Zhang. 2019. “Effects of Long-Lasting High-Definition Transcranial Direct Current Stimulation in Chronic Disorders of Consciousness: A Pilot Study.” *Frontiers in Neuroscience* 13 (April): 412.

Hermann, Bertrand, Federico Raimondo, Lukas Hirsch, Yu Huang, Mélanie Denis-Valente, Pauline Pérez, Denis Engemann, et al. 2020. “Combined Behavioral and Electrophysiological Evidence for a Direct Cortical Effect of Prefrontal tDCS on Disorders of Consciousness.” *Scientific Reports* 10 (1): 4323.

Hindriks, R., M. H. Adhikari, Y. Murayama, M. Ganzetti, D. Mantini, N. K. Logothetis, and G. Deco. 2016. “Can Sliding-Window Correlations Reveal Dynamic Functional

Connectivity in Resting-State fMRI?" *NeuroImage* 127 (February): 242–56.
Hsu, Gavin, A. Duke Shereen, Leonardo G. Cohen, and Lucas C. Parra. 2023. "Robust Enhancement of Motor Sequence Learning with 4 mA Transcranial Electric Stimulation." *Brain Stimulation* 16 (1): 56–67.
Huang, Wangshan, Sarah Wannez, Felipe Fregni, Xiaohua Hu, Shan Jing, Geraldine Martens, Minhui He, Haibo Di, Steven Laureys, and Aurore Thibaut. 2017. "Repeated Stimulation of the Posterior Parietal Cortex in Patients in Minimally Conscious State: A Sham-Controlled Randomized Clinical Trial." *Brain Stimulation* 10 (3): 718–20.
Huang, Yu, Yuzhuo Su, Christopher Rorden, Jacek Dmochowski, Abhishek Datta, and Lucas C. Parra. 2012. "An Automated Method for High-Definition Transcranial Direct Current Stimulation Modeling." *Conference Proceedings: ... Annual International Conference of the IEEE Engineering in Medicine and Biology Society. IEEE Engineering in Medicine and Biology Society. Conference* 2012: 5376–79.
Huang, Zirui, Jun Zhang, Jinsong Wu, George A. Mashour, and Anthony G. Hudetz. 2020. "Temporal Circuit of Macroscale Dynamic Brain Activity Supports Human Consciousness." *Science Advances* 6 (11): eaaz0087.
Kajimura, Shogo, and Michio Nomura. 2015. "Decreasing Propensity to Mind-Wander with Transcranial Direct Current Stimulation." *Neuropsychologia* 75 (August): 533–37.
Karahanoğlu, Fikret Işik, and Dimitri Van De Ville. 2015. "Transient Brain Activity Disentangles fMRI Resting-State Dynamics in Terms of Spatially and Temporally Overlapping Networks." *Nature Communications* 6 (July): 7751.
Kato, Risako, and Ken Solt. 2021. "Prehabilitation With Brain Stimulation?" *Anesthesia and Analgesia*.
Keeser, Daniel, Thomas Meindl, Julie Bor, Ulrich Palm, Oliver Pogarell, Christoph Mulert, Jerome Brunelin, Hans-Jürgen Möller, Maximilian Reiser, and Frank Padberg. 2011. "Prefrontal Transcranial Direct Current Stimulation Changes Connectivity of Resting-State Networks during fMRI." *The Journal of Neuroscience: The Official Journal of the Society for Neuroscience* 31 (43): 15284–93.
Kötter, Rolf, and Egon Wanke. 2005. "Mapping Brains without Coordinates." *Philosophical Transactions of the Royal Society of London. Series B, Biological Sciences* 360 (1456): 751–66.
Krone, Lukas, Lukas Frase, Hannah Piosczyk, Peter Selhausen, Sulamith Zittel, Friederike Jahn, Marion Kuhn, et al. 2017. "Top-down Control of Arousal and Sleep: Fundamentals and Clinical Implications." *Sleep Medicine Reviews* 31 (February): 17–24.
Kuo, Hsiao-I, Marom Bikson, Abhishek Datta, Preet Minhas, Walter Paulus, Min-Fang Kuo, and Michael A. Nitsche. 2013. "Comparing Cortical Plasticity Induced by Conventional and High-Definition 4 × 1 Ring tDCS: A Neurophysiological Study." *Brain Stimulation* 6 (4): 644–48.
Leaver, Amber M., Sara Gonzalez, Megha Vasavada, Antoni Kubicki, Mayank Jog, Danny J. J. Wang, Roger P. Woods, et al. 2022. "Modulation of Brain Networks during MR-Compatible Transcranial Direct Current Stimulation." *NeuroImage* 250 (April): 118874.
Lefaucheur, Jean-Pascal, Andrea Antal, Samar S. Ayache, David H. Benninger, Jérôme

Brunelin, Filippo Cogiamanian, Maria Cotelli, et al. 2017. “Evidence-Based Guidelines on the Therapeutic Use of Transcranial Direct Current Stimulation (tDCS).” *Clinical Neurophysiology: Official Journal of the International Federation of Clinical Neurophysiology* 128 (1): 56–92.

Lefaucheur, Jean-Pascal, and Fabrice Wendling. 2019. “Mechanisms of Action of tDCS: A Brief and Practical Overview.” *Neurophysiologie Clinique = Clinical Neurophysiology* 49 (4): 269–75.

Liu, Zhenyu, Xintong Zhang, Binbin Yu, Jiayue Wang, and Xiao Lu. 2023. “Effectiveness on Level of Consciousness of Non-Invasive Neuromodulation Therapy in Patients with Disorders of Consciousness: A Systematic Review and Meta-Analysis.” *Frontiers in Human Neuroscience* 17 (May): 1129254.

Louviot, Samuel, Louise Tyvaert, Louis G. Maillard, Sophie Colnat-Coulbois, Jacek Dmochowski, and Laurent Koessler. 2022. “Transcranial Electrical Stimulation Generates Electric Fields in Deep Human Brain Structures.” *Brain Stimulation* 15 (1): 1–12.

Luppi, Andrea I., Daniel Golkowski, Andreas Ranft, Rüdiger Ilg, Denis Jordan, David K. Menon, and Emmanuel A. Stamatakis. 2021. “Brain Network Integration Dynamics Are Associated with Loss and Recovery of Consciousness Induced by Sevoflurane.” *Human Brain Mapping* 42 (9): 2802–22.

Luppi, Andrea I., Lynn Uhrig, Jordy Tasserie, Camilo M. Signorelli, Emmanuel A. Stamatakis, Alain Destexhe, Bechir Jarraya, and Rodrigo Cofre. 2024. “Local Orchestration of Distributed Functional Patterns Supporting Loss and Restoration of Consciousness in the Primate Brain.” *Nature Communications* 15 (1): 2171.

Lurie, Daniel J., Daniel Kessler, Danielle S. Bassett, Richard F. Betzel, Michael Breakspear, Shella Kheilholz, Aaron Kucyi, et al. 2020. “Questions and Controversies in the Study of Time-Varying Functional Connectivity in Resting fMRI.” *Network Neuroscience (Cambridge, Mass.)* 4 (1): 30–69.

Maeoka, Hiroshi, Atsushi Matsuo, Makoto Hiyamizu, Shu Morioka, and Hiroshi Ando. 2012. “Influence of Transcranial Direct Current Stimulation of the Dorsolateral Prefrontal Cortex on Pain Related Emotions: A Study Using Electroencephalographic Power Spectrum Analysis.” *Neuroscience Letters* 512 (1): 12–16.

Mansouri, Mohammad Taghi, and Paul S. García. 2021. “Repetitive Anodal Transcranial Direct Current Stimulation Hastens Isoflurane-Induced Emergence and Recovery and Enhances Memory in Healthy Rats.” *Anesthesia and Analgesia* 132 (5): 1347–58.

Martens, Géraldine, Felipe Fregni, Manon Carrière, Alice Barra, Steven Laureys, and Aurore Thibaut. 2019. “Single tDCS Session of Motor Cortex in Patients with Disorders of Consciousness: A Pilot Study.” *Brain Injury: [BI]* 33 (13-14): 1679–83.

Martens, Géraldine, Nicolas Lejeune, Anthony Terrence O’Brien, Felipe Fregni, Charlotte Martial, Sarah Wannez, Steven Laureys, and Aurore Thibaut. 2018. “Randomized Controlled Trial of Home-Based 4-Week tDCS in Chronic Minimally Conscious State.” *Brain Stimulation* 11 (5): 982–90.

McCormick, D. A. 1992. “Neurotransmitter Actions in the Thalamus and Cerebral Cortex and Their Role in Neuromodulation of Thalamocortical Activity.” *Progress in Neurobiology* 39 (4): 337–88.

McIntire, Lindsey K., R. Andy McKinley, Chuck Goodyear, and Justin Nelson. 2014. “A Comparison of the Effects of Transcranial Direct Current Stimulation and Caffeine on Vigilance and Cognitive Performance during Extended Wakefulness.” *Brain Stimulation* 7 (4): 499–507.

Mondino, Marine, Sukhmanjit Ghumman, Claire Gane, Emmanuelle Renauld, Kevin Whittingstall, and Shirley Fecteau. 2019. “Effects of Transcranial Stimulation With Direct and Alternating Current on Resting-State Functional Connectivity: An Exploratory Study Simultaneously Combining Stimulation and Multiband Functional Magnetic Resonance Imaging.” *Frontiers in Human Neuroscience* 13: 474.

Mortaheb, Sepehr, Laurens Van Calster, Federico Raimondo, Manousos A. Klados, Paradeisios Alexandros Boulakis, Kleio Georgoula, Steve Majerus, Dimitri Van De Ville, and Athena Demertzi. 2022. “Mind Blanking Is a Distinct Mental State Linked to a Recurrent Brain Profile of Globally Positive Connectivity during Ongoing Mentation.” *Proceedings of the National Academy of Sciences of the United States of America* 119 (41): e2200511119.

Nitsche, M. A., and W. Paulus. 2000. “Excitability Changes Induced in the Human Motor Cortex by Weak Transcranial Direct Current Stimulation.” *The Journal of Physiology* 527 Pt 3 (Pt 3): 633–39.

Nitsche, Michael A., and Marom Bikson. 2017. “Extending the Parameter Range for tDCS: Safety and Tolerability of 4 mA Stimulation.” *Brain Stimulation*.

Patel, Shaun R., Jesus J. Ballesteros, Omar J. Ahmed, Pamela Huang, Jessica Briscoe, Emad N. Eskandar, and Yumiko Ishizawa. 2020. “Dynamics of Recovery from Anaesthesia-Induced Unconsciousness across Primate Neocortex.” *Brain: A Journal of Neurology* 143 (3): 833–43.

Peña-Gómez, Cleofé, Roser Sala-Lonch, Carme Junqué, Immaculada C. Clemente, Dídac Vidal, Núria Bargalló, Carles Falcón, Josep Valls-Solé, Álvaro Pascual-Leone, and David Bartrés-Faz. 2012. “Modulation of Large-Scale Brain Networks by Transcranial Direct Current Stimulation Evidenced by Resting-State Functional MRI.” *Brain Stimulation* 5 (3): 252–63.

Peng, Yuan, Jingpu Zhao, Xiao Lu, Juntao Dong, Shunxi Zhang, Jin Zhang, Huihua Liu, et al. 2022. “Efficacy of Transcranial Direct Current Stimulation Over Dorsolateral Prefrontal Cortex in Patients With Minimally Conscious State.” *Frontiers in Neurology* 13 (February): 821286.

Perri, Rinaldo Livio, and Gloria Di Filippo. 2023. “Alteration of Hypnotic Experience Following Transcranial Electrical Stimulation of the Left Prefrontal Cortex.” *International Journal of Clinical and Health Psychology: IJCHP* 23 (2): 100346.

Perri, Rinaldo L., Davide Perrotta, Francesco Rossani, and Ronald J. Pekala. 2022. “Boosting the Hypnotic Experience. Inhibition of the Dorsolateral Prefrontal Cortex Alters Hypnotizability and Sense of Agency. A Randomized, Double-Blind and Sham-Controlled tDCS Study.” *Behavioural Brain Research* 425 (May): 113833.

Polanía, Rafael, Walter Paulus, and Michael A. Nitsche. 2012. “Modulating Cortico-Striatal and Thalamo-Cortical Functional Connectivity with Transcranial Direct Current Stimulation.” *Human Brain Mapping* 33 (10): 2499–2508.

Preti, Maria Giulia, Thomas Aw Bolton, and Dimitri Van De Ville. 2017. “The Dynamic Functional Connectome: State-of-the-Art and Perspectives.” *NeuroImage* 160 (October): 41–54.

Raichle, M. E., A. M. MacLeod, A. Z. Snyder, W. J. Powers, D. A. Gusnard, and G. L. Shulman. 2001. “A Default Mode of Brain Function.” *Proceedings of the National Academy of Sciences of the United States of America* 98 (2): 676–82.

Rebollo, Beatriz, Bartosz Telenczuk, Alvaro Navarro-Guzman, Alain Destexhe, and Maria V. Sanchez-Vives. 2021. “Modulation of Intercolumnar Synchronization by Endogenous Electric Fields in Cerebral Cortex.” *Science Advances* 7 (10). https://doi.org/10.1126/sciadv.abc7772.

Roncero, Carlos, Michal Friedman, Kayla Whittaker, Alex Popov, and Howard Chertkow. 2021. “Administration of 4 mA tDCS to a Person with Progressive Supranuclear Palsy Leads to Improved Walking Speed.” *Brain Stimulation* 14 (6): 1563–65.

Saturnino, Guilherme B., Oula Puonti, Jesper D. Nielsen, Daria Antonenko, Kristoffer H. Madsen, and Axel Thielscher. 2019. “SimNIBS 2.1: A Comprehensive Pipeline for Individualized Electric Field Modelling for Transcranial Brain Stimulation.” In *Brain and Human Body Modeling: Computational Human Modeling at EMBC 2018*, edited by Sergey Makarov, Marc Horner, and Gregory Noetscher. Cham (CH): Springer.

Shannon, C. E. 1948. *A mathematical theory of communication*.

Shen, Kelly, Gleb Bezgin, Michael Schirner, Petra Ritter, Stefan Everling, and Anthony R. McIntosh. 2019. “A Macaque Connectome for Large-Scale Network Simulations in TheVirtualBrain.” *Scientific Data* 6 (1): 123.

Shine, James M., Patrick G. Bissett, Peter T. Bell, Oluwasanmi Koyejo, Joshua H. Balsters, Krzysztof J. Gorgolewski, Craig A. Moodie, and Russell A. Poldrack. 2016. “The Dynamics of Functional Brain Networks: Integrated Network States during Cognitive Task Performance.” *Neuron* 92 (2): 544–54.

Steriade, Mircea M., and Robert W. McCarley. 2013. *Brainstem Control of Wakefulness and Sleep*. Springer Science & Business Media.

Straudi, Sofia, Valentina Bonsangue, Sonia Mele, Laila Craighero, Andrea Montis, Felipe Fregni, Susanna Lavezzi, and Nino Basaglia. 2019. “Bilateral M1 Anodal Transcranial Direct Current Stimulation in Post Traumatic Chronic Minimally Conscious State: A Pilot EEG-tDCS Study.” *Brain Injury: [BI]* 33 (4): 490–95.

Tagliazucchi, Enzo, and Helmut Laufs. 2014. “Decoding Wakefulness Levels from Typical fMRI Resting-State Data Reveals Reliable Drifts between Wakefulness and Sleep.” *Neuron* 82 (3): 695–708.

Tasserie, Jordy, Lynn Uhrig, Jacobo D. Sitt, Dragana Manasova, Morgan Dupont, Stanislas Dehaene, and Béchir Jarraya. 2022. “Deep Brain Stimulation of the Thalamus Restores Signatures of Consciousness in a Nonhuman Primate Model.” *Science Advances* 8 (11): eabl5547.

Thibaut, Aurore, Marie-Aurélie Bruno, Didier Ledoux, Athena Demertzi, and Steven Laureys. 2014. “tDCS in Patients with Disorders of Consciousness: Sham-Controlled Randomized Double-Blind Study.” *Neurology* 82 (13): 1112–18.

Thibaut, Aurore, Felipe Fregni, Anna Estraneo, Salvatore Fiorenza, Enrique Noe, Roberto Llorens, Joan Ferri, et al. 2023. “Sham-Controlled Randomized Multicentre Trial of Transcranial Direct Current Stimulation for Prolonged Disorders of Consciousness.” *European Journal of Neurology: The Official Journal of the European Federation of Neurological Societies* 30 (10): 3016–31.

Thibaut, Aurore, Sarah Wannez, Anne-Francoise Donneau, Camille Chatelle, Olivia

Gosseries, Marie-Aurélie Bruno, and Steven Laureys. 2017. “Controlled Clinical Trial of Repeated Prefrontal tDCS in Patients with Chronic Minimally Conscious State.” *Brain Injury: [BI]* 31 (4): 466–74.

Uhrig, Lynn, Stanislas Dehaene, and Béchir Jarraya. 2014. “A Hierarchy of Responses to Auditory Regularities in the Macaque Brain.” *The Journal of Neuroscience: The Official Journal of the Society for Neuroscience* 34 (4): 1127–32.

Uhrig, Lynn, David Janssen, Stanislas Dehaene, and Béchir Jarraya. 2016. “Cerebral Responses to Local and Global Auditory Novelty under General Anesthesia.” *NeuroImage* 141 (November): 326–40.

Uhrig, Lynn, Jacobo D. Sitt, Amaury Jacob, Jordy Tasserie, Pablo Barttfeld, Morgan Dupont, Stanislas Dehaene, and Bechir Jarraya. 2018. “Resting-State Dynamics as a Cortical Signature of Anesthesia in Monkeys.” *Anesthesiology* 129 (5): 942–58.

Vincent, Justin L., Abraham Z. Snyder, Michael D. Fox, Benjamin J. Shannon, Jessica R. Andrews, Marcus E. Raichle, and Randy L. Buckner. 2006. “Coherent Spontaneous Activity Identifies a Hippocampal-Parietal Memory Network.” *Journal of Neurophysiology* 96 (6): 3517–31.

Virtanen, Pauli, Ralf Gommers, Travis E. Oliphant, Matt Haberland, Tyler Reddy, David Cournapeau, Evgeni Burovski, et al. 2020. “SciPy 1.0: Fundamental Algorithms for Scientific Computing in Python.” *Nature Methods* 17 (3): 261–72.

Vohryzek, Jakub, Gustavo Deco, Bruno Cessac, Morten L. Kringelbach, and Joana Cabral. 2020. “Ghost Attractors in Spontaneous Brain Activity: Recurrent Excursions Into Functionally-Relevant BOLD Phase-Locking States.” *Frontiers in Systems Neuroscience* 14 (April): 20.

Wan, Xiaoping, Yong Wang, Ye Zhang, and Weiqun Song. 2023. “A Comparison of the Neuromodulation Effects of Frontal and Parietal Transcranial Direct Current Stimulation on Disorders of Consciousness.” *Brain Sciences* 13 (9). https://doi.org/10.3390/brainsci13091295.

Wirth, Miranka, Rasha Abdel Rahman, Janina Kuenecke, Thomas Koenig, Helge Horn, Werner Sommer, and Thomas Dierks. 2011. “Effects of Transcranial Direct Current Stimulation (tDCS) on Behaviour and Electrophysiology of Language Production.” *Neuropsychologia* 49 (14): 3989–98.

Wu, Min, Yamei Yu, Lunjie Luo, Yuehao Wu, Jian Gao, Xiangming Ye, and Benyan Luo. 2019. “Efficiency of Repetitive Transcranial Direct Current Stimulation of the Dorsolateral Prefrontal Cortex in Disorders of Consciousness: A Randomized Sham-Controlled Study.” *Neural Plasticity* 2019 (June): 7089543.

Xie, Hua, Javier Gonzalez-Castillo, Daniel A. Handwerker, Peter A. Bandettini, Vince D. Calhoun, Gang Chen, Eswar Damaraju, Xiangyu Liu, and Sunanda Mitra. 2019. “Time-Varying Whole-Brain Functional Network Connectivity Coupled to Task Engagement.” *Network Neuroscience (Cambridge, Mass.)* 3 (1): 49–66.

Xu, Zeyu, Ruizhe Zheng, Tiantong Xia, Zengxin Qi, Di Zang, Zhe Wang, and Xuehai Wu. 2022. “Behavioral Effects in Disorders of Consciousness Following Transcranial Direct Current Stimulation: A Systematic Review and Individual Patient Data Meta-Analysis of Randomized Clinical Trials.” *Frontiers in Neurology* 13 (September): 940361.

Zhang, Chunyun, Shuai Han, Zean Li, Xinjun Wang, Chuanxiang Lv, Xiangyun Zou, Fulei Zhu, et al. 2022. “Multidimensional Assessment of Electroencephalography in

the Neuromodulation of Disorders of Consciousness." *Frontiers in Neuroscience* 16 (June): 903703.

Zhang, Ye, Weiqun Song, Jubao Du, Su Huo, Guixiang Shan, and Ran Li. 2017. "Transcranial Direct Current Stimulation in Patients with Prolonged Disorders of Consciousness: Combined Behavioral and Event-Related Potential Evidence." *Frontiers in Neurology* 8 (November): 620.

Yiheng Tu, Jin Cao, Seyhmus Guler, Thalia Chai-Zhang, Joan A. Camprodon, Mark Vangel, Randy L. Gollub, Darin D. Dougherty, Jian Kong. "Perturbing fMRI brain dynamics using transcranial direct current stimulation." NeuroImage, Volume 237, 2021. 118100, ISSN 1053-8119. https://doi.org/10.1016/j.neuroimage.2021.118100.